REDUCING STAKEHOLDER VULNERABILITY TO CLIMATE VARIABILITY IN SOUTHERN PERU USING STATISTICALLY-BASED PREDICTION AND RISK MANAGEMENT TOOLS

Written By:

Eric Scott Mortensen

A thesis submitted in partial fulfillment

of the requirements for the degree of

MASTER OF SCIENCE

CIVIL AND ENVIROMENTAL ENGINEERING

at the

UNIVERSITY OF WISCONSIN – MADISON

Submitted December 2017

ACKNOWLEDGEMENTS

I would like to thank my graduate advisor, Dr. Paul Block, for his continual support and guidance throughout the course of my graduate studies at the University of Wisconsin – Madison. His willingness to let me explore challenging topics and eagerness to see me succeed in doing so has allowed me to grow personally and professionally in ways otherwise implausible.

I would also like to give thanks to the other two members of my committee, Dr. Stephen Vavrus and Dr. Daniel Wright, for their insights and feedback on my research as it has progressed during the past several years.

The research presented in this thesis was funded by Southern Peru Copper Corporation as well as the Climate, People, and the Environment Program of the Nelson Institute Center for Climatic Research. Special thanks are given to the dedicated team members of these organizations who chose to support this research.

In addition, this research would be largely infeasible without support from several individuals and organizations including: Mr. José de Piérola; Mr. Rob Montgomery; Dr. Michael Notaro; Dr. Shu Wu; Servicio Nacional de Meteorología e Hidrología del Perú; Autoridad Nacional del Agua; Red Cross Red Crescent Climate Centre; Ministerio de Agricultura y Riego; and many, many more.

Finally, wholehearted thanks are given to my colleagues, friends, and family members for brightening my life and tolerating my hectic lifestyle over the past several years of my time as a graduate student at the University of Wisconsin – Madison. Your loyalty and generosity mean the world to me, and I value your presence in my life greatly.

ABSTRACT

Located at a complex topographic, climatic, and hydrologic crossroads, southern Peru is a semi-arid region that exhibits high spatiotemporal variability in precipitation. The economic viability of the region hinges on this water, yet southern Peru is prone to water scarcity caused by seasonal meteorological drought. Agricultural operations in southern Peru are particularly vulnerable to drought, and the response to drier than normal conditions in this region can be characterized as reactive and fairly limited due to challenges associated with climate forecasting and administrative capacity. Meteorological droughts in this region here are often triggered during El Niño episodes and have direct hydrologic, economic, and social implications. To reduce the vulnerability faced across several sectors, statistically-based tools are developed to predict drought and provide additional resources to stakeholders.

An extensive season-ahead precipitation prediction model is developed and conditioned on ENSO and other large-scale climate mechanisms. In addition to existing climate indices, large-scale climatic variables, such as sea surface temperature, are investigated to identify potential drought predictors. A principal component regression framework is applied to eleven potential predictors to produce an ensemble forecast of regional January-March precipitation totals. Model hindcasts of 51 years, compared to climatology and another model conditioned solely on an El Niño-Southern Oscillation index, achieve notable skill and perform better for several metrics, including ranked probability skill score and a hit-miss statistic. Extending the lead time of and spatially disaggregating precipitation predictions to the local level as well as forecasting the number of wet/dry days per rainy season may further assist regional stakeholders and policymakers in preparing for drought.

An ENSO index-based insurance product is also presented as a demonstration of methodology and application for oca production in Puno of southern Peru. The purpose of this product is to streamline the ability of decision makers to provide financial relief to affected farmers during, and perhaps before, drought; extending the lead time of the index used to trigger payouts produces results of similar skill to a product trained on concurrent conditions. Issues explored include basis risk, initial endowment requirements, product longevity, and the potential crossover from index-based insurance to forecast-based financing. The potential for uptake of such products is real in Peru, and of considerable interest to both regional government and relief agencies

TABLE OF CONTENTS

CHATPER 1: INTRODUCTION AND CONTEXT

Southern Peru is a semi-arid region just north of the Atacama Desert, located at a complex topographic, climatic, and hydrologic crossroads. With elevations ranging from sea level to over 6,000 meters, the area is a patchwork of snow-capped Andean mountains, highlands and plateaus, and large expanses of coastal desert. Due to its proximity to the Amazon rainforest, the Atacama Desert, and the Pacific Ocean, the climate patterns that govern the region's precipitation vary considerably, both seasonally and annually. Although a notable portion of this region drains to Lake Titicaca, which is itself a part of a larger endorheic basin, the majority of the region's water flows into the Pacific Ocean through networks of small rivers and quebradas, or seasonal creeks. While the topographic, climatic, and hydrologic factors of the region produce spatiotemporal variability in the distribution of water resources (Tapley and Waylen, 1990), southern Peru can be characterized as water scarce (Alegría, 2006; Kuroiwa, 2007; Ugarte, 2012; Chinchay Alza, 2015).

Nonetheless, southern Peru displays a high economic dependence on activities driven directly by water availability, specifically agriculture and mining (Higa Eda and Chen, 2010). The region is home to a flourishing agricultural sector, as well as several large-scale copper mining operations. Both of these industries are heavily dependent on water consumption. Additionally, several large urban areas such as Arequipa, Juliaca, and Tacna necessarily require large quantities of water to thrive as economic and cultural centers.

Agriculture is a particularly important sector to the country of Peru, accounting for roughly 8% of national GDP and 25% of the labor force (Peterson, 2015). The 2.2 million farmers of Peru produce one of the most diverse spreads of crop in the world. This indeed is the case in southern Peru, a region composed of four departments (Arequipa, Moquegua, Puno, and Tacna) that produced more than 1.25 million tons of crop in 2014 (Chiock Chang, 2016). The main crops produced in this region include tree fruits, tubers, alfalfa, and common vegetables. Southern Peru, however, is also home to some of the nation's richest grapevine fields that are used for Peru's signature pisco brandy, certain non-traditional agricultural exports, and several endemic crops relied upon for centuries by indigenous groups. The agricultural operations of the region are varied, ranging from groundwater pumping-intensive operations near the coast, to irrigated farms along small seasonal rivers, and also rain-fed fields in the highlands (Velazco, 2001). While there are some large-scale commercial operations responsible for a large portion of the region's exports to other parts of the

country, more than 60% of farmers in southern Peru cultivate less than 3 hectares of land (Vera, 2006) and participate in a fairly localized market. Additionally, two-thirds of these farms are rain-fed (Robles, 2015). Such factors are relevant when considering the impact of meteorological drought on a semi-arid region participating in economic activities dependent on water availability.

Although not equivalent, meteorological drought in this region often directly translates into hydrologic drought (Van Loon, 2015). Droughts, like the one that struck in early 2016, have a critical impact on the success and survival of the region. During that year, agricultural outputs of southern Peru were reduced by up to 75% (ANA, 2016), necessitating the creation of an emergency contingency fund for impacted farmers by Peru's national water authority (in Spanish, Autoridad Nacional del Agua, or ANA). ANA also declared states of emergency for two cities, Tacna and Arequipa. Consequentially, the cities' water supplies were reduced by more than one-fourth. The mining operations of the region were also negatively impacted, with ANA ordering mining companies such as Southern Peru Copper Corporation (SPCC), to reduce their water consumption and, transitively, copper production, resulting in lost economic potential and reduced fiscal resources for the region as a whole.

The severity of this most recent bout of drought, unfortunately, is not unprecedented; other droughts in the past have also caused serious economic and social consequences. The drought event of early 1983 was particularly severe across southern Peru (Caviedes, 1985). Before this event, hazard preparedness essentially did not exist in Peru. The drought, which coincided with deadly flooding in the northern part of the country, was generally met with slow and uncoordinated official disaster relief. Even after the country developed their national hazard preparedness program (immediately following the 1983 event), the region continues to be vulnerable to drought. In 1998, an estimated $200 million in direct losses occurred over the southern Andes of Peru due to drought (Lavado-Casimiro et al., 2013).

One unfamiliar with the region might expect an array of well-established and pervasive predictive tools and insurance products readily available for use by stakeholders within the region to reduce deleterious impacts of drought; however, the reality of climate prediction and insurance in southern Peru is not as sanguine as this scenario. Current climate modeling efforts undertaken by the national meteorological service (in Spanish, Servicio Nacional de Meteorología e Hidrología del Perú, or SENAMHI) are more oriented towards monitoring and short-term forecasting. And while

one insurance product is currently offered by the Peruvian company La Positiva Seguros on a nationwide basis against catastrophic losses (Peña Henderson, 2016), only 8% of farmers in southern Peru have adequate credit to acquire such a product (Robles, 2015).

The challenges created by drought, when combined with other factors such as cultural differences and socioeconomic disparities, can instigate economic instability and societal stress regionally (Lynch, 2012). While tools exist to monitor drought and hydroclimatic conditions, such as the Peruvian Drought Observatory (ANA, 2014), and provide financial resources via traditional insurance products, other statistically-based tools remain relatively unexplored for southern Peru. If droughts could be predicted several months or seasons in advance, regional decision makers, private entities, local interests, and other stakeholders may be able to reduce their immediate vulnerability to hydroclimatic variability in the form of water planning and resource distribution (Sadoff and Muller, 2009). Season-ahead drought prediction and agricultural insurance products may afford stakeholders more capacity to address mid- and long-term water resources planning issues and goals (Ugarte, 2012; Chinchay Alza, 2015).

A statistically-based season-ahead principal component regression (PCR) model that predicts seasonal precipitation totals is developed to address this existing gap. The PCR model draws on a far-reaching pool of large-scale climate variables that influence southern Peru precipitation through ocean-atmosphere teleconnections. The model is evaluated against climatology and simpler ENSO index-based models to understand if the inclusion of several predictors leads to more skillful prediction, particularly for dry years in this drought-sensitive region. In addition, several ancillary applications of this model are explored, including lead time extension, spatial disaggregation, and wet/dry day frequency prediction, in an attempt to provide further detailed information which may be relevant to stakeholders.

In addition, the potential for an insurance product conditioned on a climate index to reduce agricultural vulnerability to regional drought in southern Peru is explored. This risk transferring product is based on a tamper-proof index, financially self-sustaining, and not cost-prohibitive, among other advantages. The design process of the insurance framework (including the optimization of an initial endowment fund amount and payment scheme) is detailed in addition to an analysis of the results of an array of potential products. The goal of this product is to provide farmers of southern Peru a tool to use to improve their resilience to drought.

CHAPTER 2: SEASON-AHEAD PRECIPITATION PREDICTION

Data Description.

Monthly precipitation data are available for 29 stations distributed across the region over a period of 51 years (1966-2016; Fig. 1). Six of the 29 stations are owned and operated by SPCC, with the remaining stations belonging to Peru's national meteorological service (in Spanish, Servicio Nacional de Meteorologia e Hidrologia del Peru, or SENAMHI).

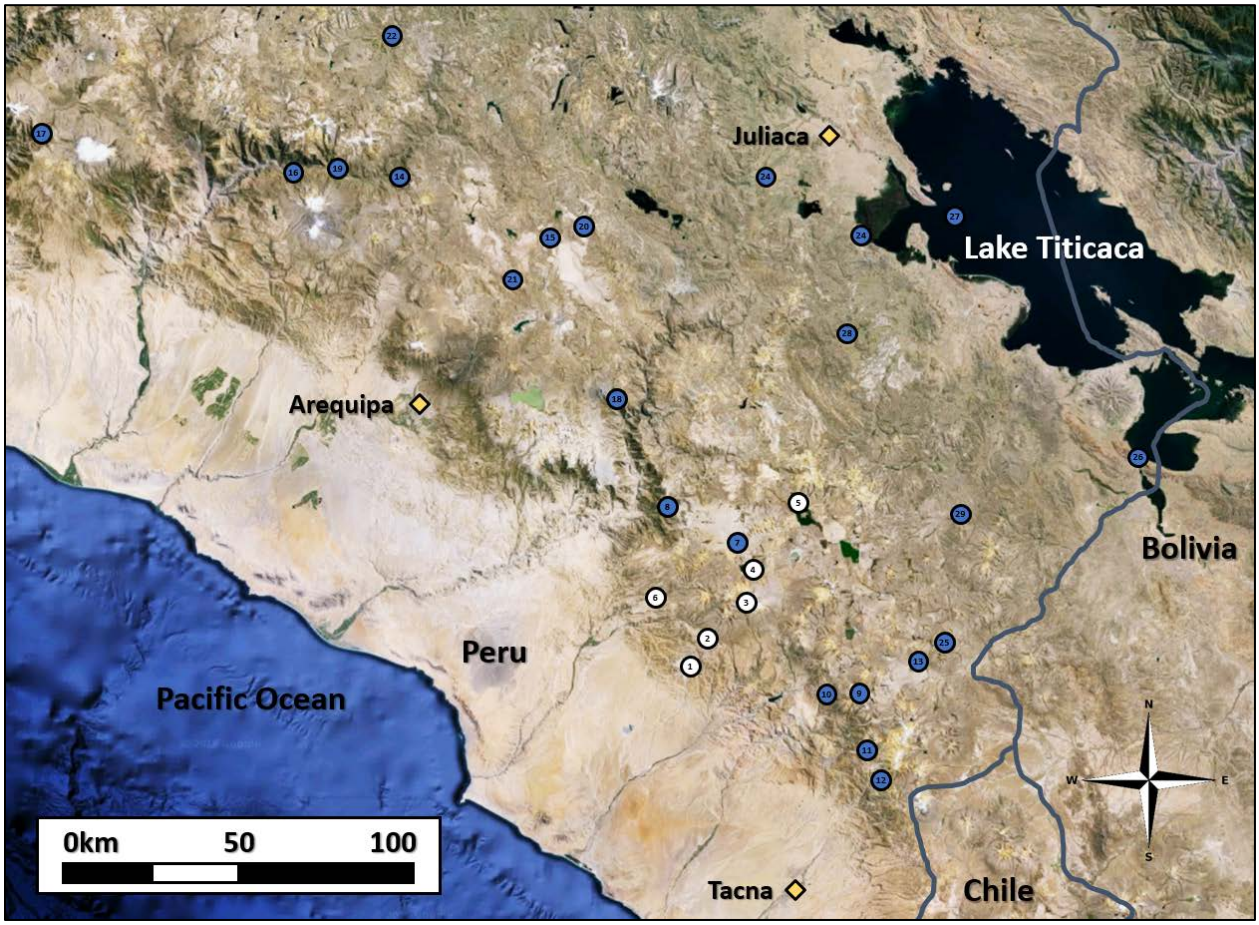

Figure 1: White circles represent locations of SPCC stations; blue circles represent SENAMHI stations. Three major urban centers are labeled and stations are numbered from 1-29 (map generated using Google Earth imagery and station information from SPCC).

The 29 stations provide spatial coverage for an area of 65,000 km^2 and are located in a variety of environments, including the edge of the Atacama Desert, the islands of Lake Titicaca, the dry grassy plains of the Altiplano, and the mountainous terrain of the Central Andes. The topography of the region is noteworthy. While the 29 stations considered in the study cover an elevation range

from 3,100 m to 4,600 m (Fig. 2, mean elevation 3870 m), this portion of southern Peru ranges from sea level at the Pacific Ocean to over 6,000 m in the high Andes.

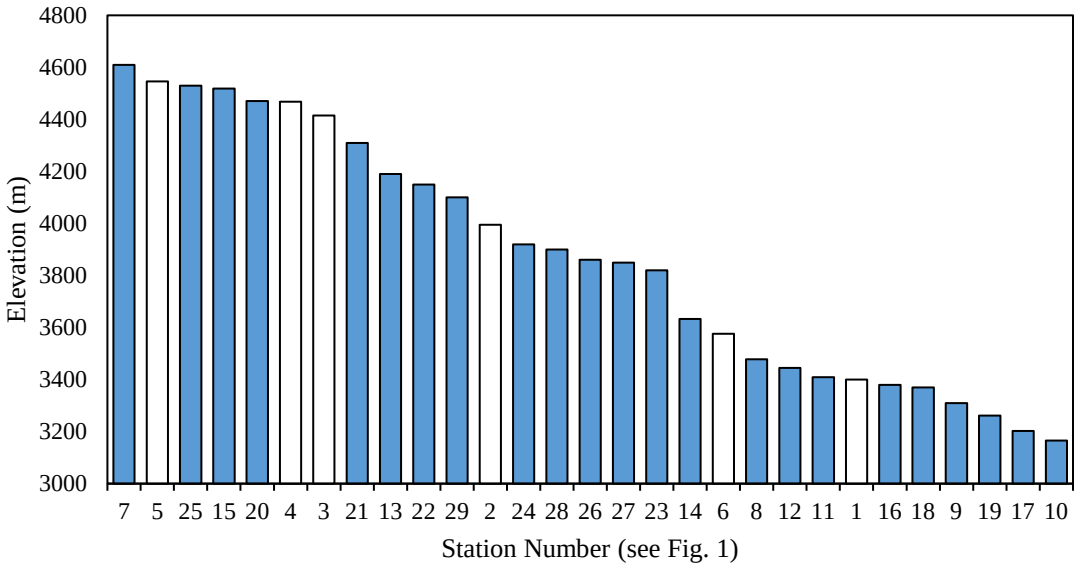

Figure 2: Elevations of all 29 stations included in the study. Bars are numbered and colored in accordance with Fig. 1, with white bars representing SPCC stations and blue bars representing SENAMHI stations.

Cross-correlations between all of the stations were calculated based on each station's available monthly precipitation totals (average Pearson's correlation coefficient, r=0.92). For any missing station data (<1% of total data), the ten most highly correlated stations were identified, and multiple regression based on monthly statistics was used to interpolate a probable missing value. In most cases, high correlation coefficients between estimated missing points and observed data suggest that this simple methodology is effective in filling the data.

Potential large-scale climate predictors, including sea surface temperature (SST), sea level pressure (SLP), and geopotential height (GH), were retrieved from the National Oceanic and Atmospheric Administration (NOAA) Earth System Research Laboratory Physical Sciences Division (ESRL-PSD). The data are based on National Centers for Environmental Prediction-National Center for Atmospheric Research (NCEP-NCAR) reanalysis data, version 1 (Kalnay et al., 1996) and are available as monthly averages on a 2.5° x 2.5° global grid (this dataset is available in full from 1948 to present). The specific regions and periods of the aforementioned climate variables considered in this study are listed in Table 1. In addition, ESRL-PSD monthly/seasonal climate correlation and composite mapping tools are used in this analysis.

In addition to the aforementioned large-scale climate variables, several established teleconnection indices, such as Niño 3.4 (Rayner et al., 2003), Pacific Decadal Oscillation (PDO; Mantua et al., 1997), North Pacific index (NP; Trenberth and Hurrell, 1994), and Western Hemisphere Warm Pool (WHWP; Wang and Enfield, 2001), are evaluated in this study.

Southern Peru Rainy Season and Large-scale Climate Influences.

In the mid-high elevation regions of southern Peru, as in most tropical zones, the annual cycle is dominated by a wet and dry season (Fig. 3). For southern Peru, the rainy season occurs from November to April (Kuroiwa, 2007); however, the majority of precipitation in the region occurs during January, February, and March (JFM; 315 mm on average). JFM precipitation represents, on average, more than two-thirds of annual precipitation for the region, with some locations receiving up to 85% of annual precipitation during the three-month period. This precipitation is crucial to the region's economic activities and environmental stability. During the rainy season, for example, surface reservoirs and underground aquifers are replenished for multi-sectoral water resource use during the dry conditions that characterize the rest of the year. These rains also directly impact the phenology of many wild plants and agricultural operations, and are intrinsically tied to the function of seasonal creeks that drain the region. As mentioned, severe and wide-reaching economic, environmental, and societal consequences can be realized in an abnormally dry rainy season. Thus, JFM is identified as the season of interest for this study.

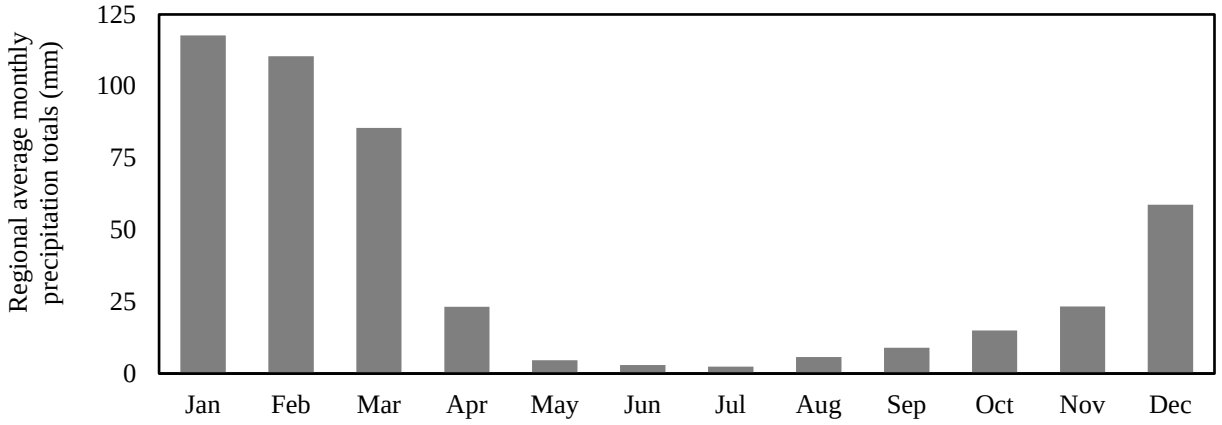

Figure 3: Average monthly precipitation (mm) of 29 stations southern Peru.

To evaluate the spatial and temporal patterns of regional precipitation, a principal component analysis (PCA) is performed on JFM seasonal precipitation totals (von Storch and Zwiers, 2001)

based on data from the 29 stations. In PCA, a dataset is decomposed into orthogonal, uncorrelated modes representing distinctive signals, or variance, present in the dataset. PCA yields information describing both spatial patterns (empirical orthogonal functions, EOFs) and temporal trends (principal components, PCs) of variance experienced in the dataset.

Even with significant changes in elevation across the region, the sign of the first EOF spatial pattern of all stations is negative (and at similar magnitudes) generally implying spatial homogeneity (Eklundh and Pilesjö, 1995; Ogallo, 1980; Mallants and Feyen, 1990; Bisetegne et al., 1986) of JFM seasonal precipitation within this relatively small region. Additionally, the first PC of the precipitation time series captures 51% of the temporal variance in the data, and correlates well with station-averaged JFM seasonal precipitation observations (r = 0.99; Fig. 4).

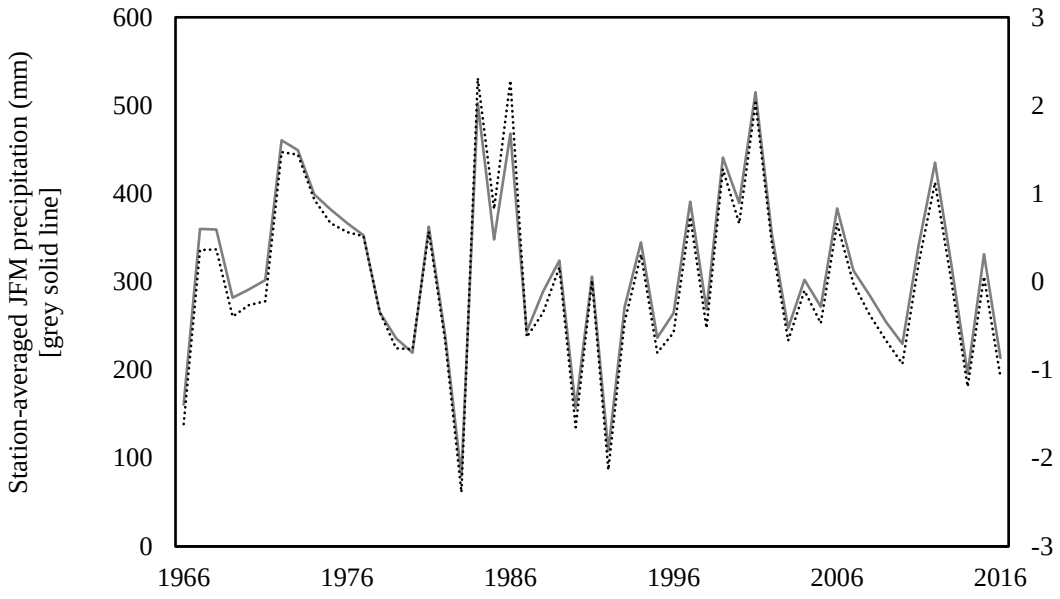

Figure 4: Station-averaged JFM precipitation (mm) and the first PC anomalies for the period of record, 1966-2016, using data from 29 precipitation stations.

This exceptional level of correlation between the averaged observations and the first PC (as well as high levels of correlation between this first PC time series and individual station data) suggest that the station-averaged time series is an appropriate representation of regional precipitation. It should be noted that the second mode captures an additional ~20% of variance, with the third dropping to ~5%. These three PCs represent a cumulative 75% of variance experienced in the dataset (it is assumed that the remaining PCs describe only minor or spurious variance). To identify

physical mechanisms that modulate precipitation that result in the observed temporal variance, the complex regional climate system must be comprehensively analyzed.

During the rainy season, the tropical Southern Hemisphere receives increased amounts of solar radiation that destabilizes the atmospheric boundary layer, inducing deep convection and moist air advection (Vuille et al., 1999; Garreaud, 1999). This directly translates to increased levels of evapotranspiration in the Amazon basin, with moisture transported deep into the atmosphere by a complex network of deep convection systems, including the upper level of the Bolivian High (Lenters and Cook, 1997). In general, the winds associated with this deep convection are easterly and northerly, carrying moisture towards the Andes from the Amazon (Fuenzalida and Rutllant, 1987; Chaffaut et al., 1998; Rao et al., 1996; Vizy and Cook, 2007). The Andes induce an orographic effect in which more precipitation occurs at windward locations and higher elevations of the region (Garreaud, 1999). Meanwhile, the precipitation at the leeward (western) side of the mountain range and lower elevations is markedly reduced; this region of southern Peru exists in the rain shadow of the Andes, a fact especially relevant for the study. Instead of an abrupt switch between wet and dry conditions as might be expected by some other notable rain shadows in the world, the Altiplano (and the majority of the stations used in this study) exists in a transitionary zone of sorts and exhibits a gradual wet to dry gradient from northeast to southwest.

Previous studies have identified SST anomalies in the equatorial Pacific as a substantial factor impacting regional precipitation patterns in southern Peru (Vuille et al., 2000; Garreaud et al. 2003; Espinoza Villar et al. 2009; Lavado-Casimiro et al., 2013; Cid-Serrano et al., 2015). This area of the Pacific is commonly associated with the El Niño-Southern Oscillation (ENSO) phenomenon, and several studies further identify the SST domain of 5° N-5° S, 120° W-170° W, known as Niño 3.4 (Trenberth, 1997), as particularly influential in modulating JFM precipitation. Strong El Niño (warm SST) conditions in the Niño 3.4 region are typically associated with drought in southern Peru, whereas La Niña (cool SST) conditions often align with wetter-than-average conditions (Fig. 5, El Niño and La Niña thresholds of 0.5°C and -0.5°C, respectively, included for context).

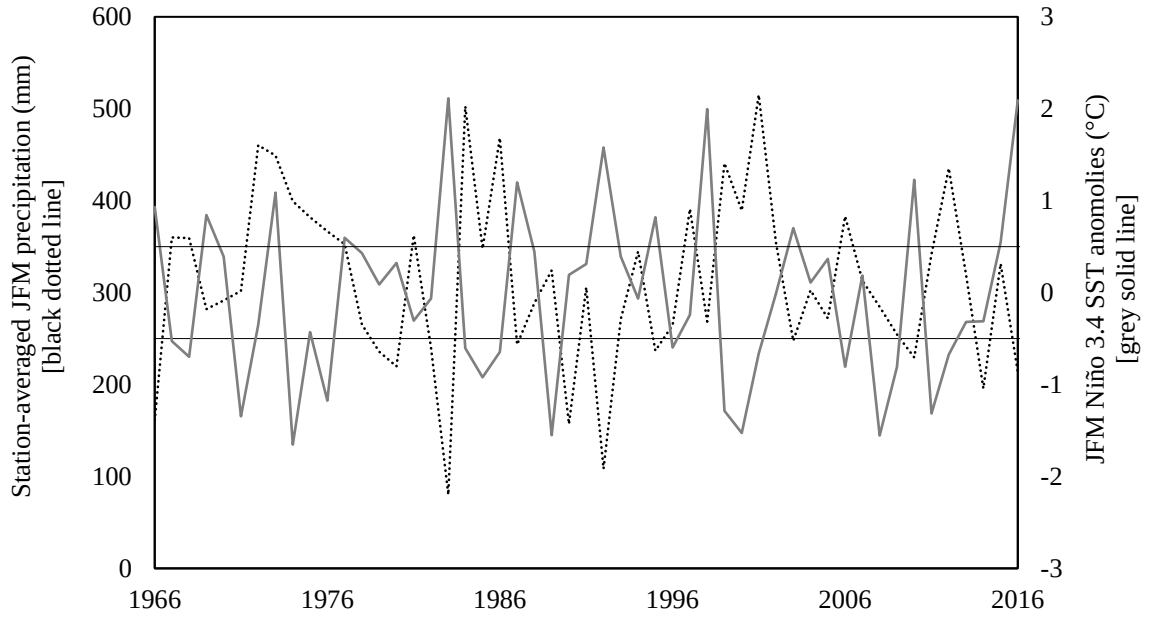

Figure 5: Station-averaged JFM precipitation and concurrent JFM Niño 3.4 SST anomalies (r=-0.57, p-value = 0.000013). El Niño and La Niña thresholds marked with black solid line. During the period of record, 13 JFMs exceeded the El Niño threshold (0.5°C) and 18 JFMs the La Niña threshold (-0.5°C).

Furthermore, prior studies have determined that droughts in southern Peru are not generally caused by limited moisture transport. During El Niño episodes, enhanced upper-level westerly flow from the Pacific Ocean weakens the typical wind patterns of the region, blocking easterly winds laden with moisture that normally falls as precipitation in southern Peru (Garreaud et al., 2003; Takahashi, 2006). During La Niña, easterly flow is enhanced, often resulting in greater precipitation and cloud cover, and lower temperatures in the central Andes (Vuille, 1999).

The phase and strength of ENSO does not necessarily correspond to a specific outcome for seasonal precipitation, a fact particularly evident in three notable cases (bolded and underlined, Fig. 6). In late 1972, a strong El Niño developed off the coast of South America; however, instead of expected dry conditions, JFM 1973 surprisingly turned out to be one of the wettest rainy seasons on record for the region (Garreaud et al., 2003). In contrast, ENSO index values indicative of neutral to weak La Niña conditions prior to JFM 1990 and 2014 would have typically been interpreted to mean normal to slightly wetter-than-average conditions, yet these years are two of the driest rainy seasons on record.

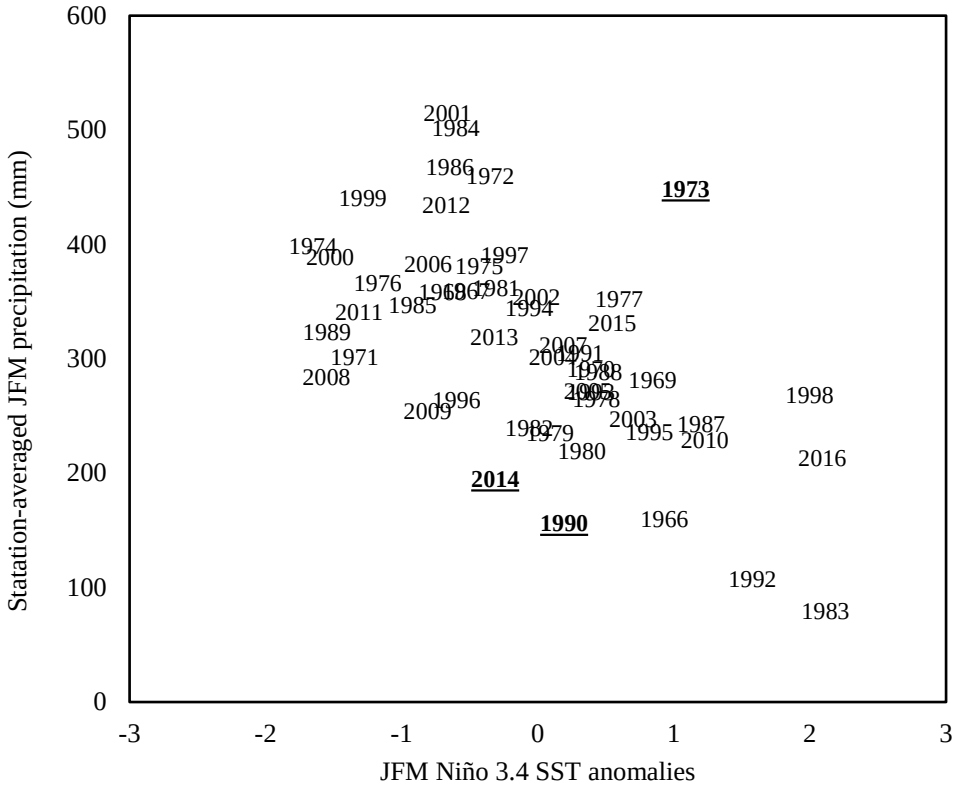

Figure 6: Three outlier years in which general relationship between Niño 3.4 and regional precipitation did not hold to be true are bolded and underlined. If the three outlier years (1973, 1990, and 2014) are removed, the relationship between precipitation and SST anomalies strengthens (r=-0.66, p-value = 0.000009).

Deviations from the generally understood relationship between ENSO and regional JFM seasonal precipitation are likely due to other climate phenomena, and support the two-fold notion of ENSO's influence on seasonal precipitation as well as the presence of additional climatic factors that modulate the region's precipitation. Regions and variables of interest highlighted in other studies (and considered in this study) as modulating mechanisms to precipitation in southern Peru include Tropical Atlantic SST, several SST regions of the Pacific, and the Bolivian High.

While the main moisture source for Altiplano precipitation is the tropical lowlands to the east of the Andes, this moisture ultimately originates over the trade wind regions of the Tropical Atlantic (Vuille et al., 2000), the primary source of moisture to the Amazon. In particular, SST anomalies in the North Tropical Atlantic regulate dry season precipitation anomalies in the western Amazon (Marengo et al., 2008; Zeng et al., 2008; Yoon and Zeng, 2010; Fernandes et al., 2011). When the North Tropical Atlantic is anomalously warm, the Intertropical Convergence Zone shifts

northward, causing net water vapor divergence, anomalous subsidence, and reduced precipitation in western/southern Amazon (Marengo, 1992; Marengo et al., 2008; Yoon and Zeng, 2010), and southern Andes (Lavado-Casimiro et al., 2012).

In the Pacific Ocean, locations outside of the traditional ENSO region also appear to impact precipitation in this region of South America. Although the subtropical Pacific is immediately adjacent to the region of interest, it typically contributes little moisture to southern Peru because low-level zonal flow and associated moisture from the sea is blocked by steep regional terrain and large-scale subsidence (Rutllant and Ulriksen, 1979). The Pacific Ocean, however, still plays a significant role in controlling the regional hydrologic cycle due to these zonal winds. The Pacific Decadal Oscillation (PDO) has also been identified as modulating precipitation throughout much of South America (Enfield, 1996; Kayano and Andreoli, 2007). This multi-decadal, low frequency oscillation of North Pacific SST impacts several regional climate systems and has been widely accepted by the hydrometeorological community as being distinct from ENSO (Deser and Blackmon, 1995; Mantua and Hare, 2002; Wang et al., 2008). Additionally, the Western Hemisphere Warm Pool (WHWP), a region of abnormally warm SST off the coast of Central America with lobes in the Caribbean and Pacific Ocean, may likewise influence regional precipitation as a result to the warming cycle's impact on rainy season precipitation in equatorial Central and South America via tradewind modulation (Wang and Enfield, 2003; Wang and Enfield, 2006). Finally, the North Pacific (NP) index, which describes SST and SLP variability in the North Pacific, has a direct connection with changes to Tropical Pacific SST and circulation patterns (Trenberth and Hurrell, 1994). PDO, WHWP, and NP indices are considered in this study.

The upper-level Bolivian High, located over the Altiplano during December-April, is related to latent heat release over the Amazon (Silva Dias et al., 1983; Lenters and Cook, 1997). The position and strength of the High has been linked to precipitation anomalies over the Altiplano during the rainy season. Specifically, a weakened, northward shifted Bolivian High is often associated with persistent dryness on the Altiplano (Aceituno and Montecinos, 1993; Lenters and Cook, 1999; Vuille et al., 2000), whereas a strong, southward shifted Bolivian High favors deep convection on the Altiplano and increased moisture availability (Garreaud and Aceituno, 2001; Garreaud et al., 2003). Thus, the position of the Bolivian High impacts zonal winds during the Altiplano's rainy

season; dry (wet) conditions over the Altiplano are associated with anomalous westerly (easterly) flow in the region (Aceituno and Montecinos, 1993; Lenters and Cook, 1999).

While the first EOF of regional precipitation likely illustrates ENSO's influence on regional precipitation, it is possible that higher order modes may describe other climatic and topographic forcings. These may include interconnected large-scale climatic phenomena or observed orographic effects. For example, the second EOF exhibits a dipole pattern of precipitation, which may be related to the rain shadow phenomenon that causes the northeastern portion of the region to be wet and southwestern dry.

Identification of Seasonal Precipitation Predictors.

Potential predictors of JFM precipitation are identified by analyzing persistent large-scale and local climate variables in the prior season of October–December (OND) based on the suite of variables and indices identified previously and validated through correlation mapping, composite mapping, and global wavelet analysis. The purpose of these three methods is to identify climate variables and indices that partially explain the variance in JFM precipitation and as a result may serve as potentially skillful predictors in the development of a season-ahead precipitation prediction model.

Spatial correlation maps between the first three PCs of JFM regional precipitation (explaining approximately 75% of the variance) and global OND climatic variables, including SST, SLP, and GH at 200 hPa, illustrate distinct regions of correlation and potentially relevant teleconnections. Only December values are used for SLP and GH given their limited atmospheric persistence. For example, the correlation between OND SST and the first PC of JFM regional precipitation produces a pattern emblematic of the classic ENSO phenomenon (Fig. 7). The area near (but not exactly) Niño 3.4 has the strongest correlation (r=-0.54), indicative of a relationship in which, generally, abnormally warm (cool) water in this region corresponds with dry (wet) conditions in southern Peru, supporting previous findings.

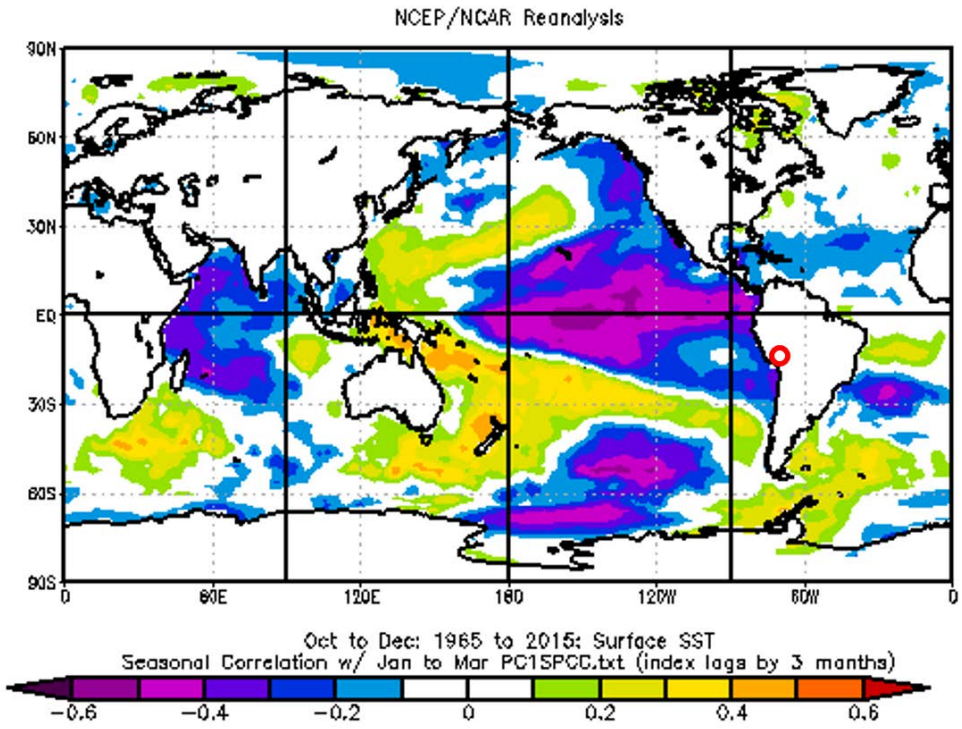

Figure 7: Correlation between global OND SST and first PC of regional JFM precipitation. Study region identified with red circle.

Not all regions, however, that display relatively high correlations with the PCs are necessarily physically relevant. To limit spurious correlations, only regions of statistical significance at the 95% confidence level and justifiable (via relevant, peer-reviewed literature) physical influence on moisture transportation to southern Peru are selected as potential predictors. Additional areas of interest identified through spatial correlation mapping include an area of SLP off the western coast of Mexico/USA (roughly 35° N-20° N, 150° W-135° W) and an area of geopotential height above southern Bolivia/northern Argentina (roughly 10° S-15° S, 70° W-65° W). These two areas, in addition to the mentioned region of SST in the equatorial Pacific, display statistical significance at the 95% confidence level to at least one of the three analyzed PCs. It can be speculated that these two regions of high correlation likely have a physical relation to the WHWP and Bolivian High, respectively.

Composite maps illustrate climate conditions for a single period or subset of periods, and may be especially useful for understanding forcing mechanisms in anomalous periods. For example, OND SST for the nine subsequent driest JFM seasons on record for southern Peru subtracted from OND SST for the nine subsequent wettest JFM seasons on record for southern Peru produce large

positive anomalies in the equatorial Pacific Ocean. This composite map (Fig. 8) further indicates the potential importance of ENSO in explaining JFM precipitation variability in the study region.

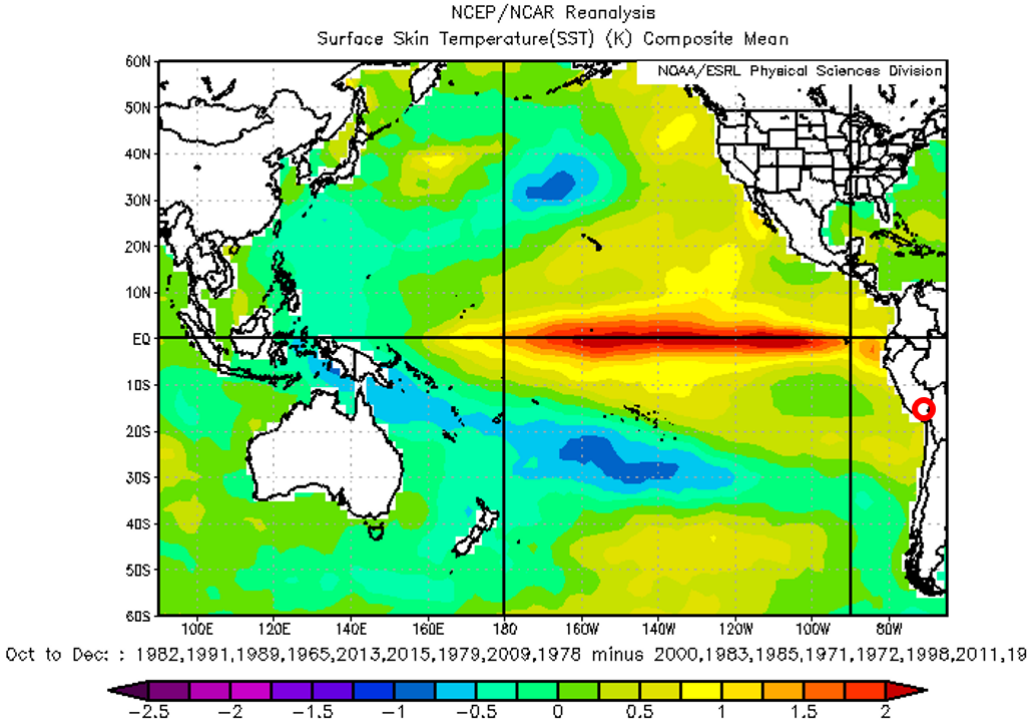

Figure 8: SST conditions for OND seasons following the nine driest JFM seasons (1983, 1992, 1990, 1966, 2014, 2016, 1980, 2010, and 1979) subtracted from SST conditions for OND seasons following the nine wettest JFM seasons (2001, 1984, 1986, 1972, 1973, 1999, 2012, 1974, and 1997). Study region identified with red circle.

Additional composite maps, namely subsets of years with the strongest El Niño and La Niña years or years with wetter-than-average El Niño years and drier-than-average La Niña years, led to identification of ENSO, SST gradients in the North Pacific and Tropical Atlantic Oceans, and the Pacific lobe of the WHWP as potentially skillful predictors of JFM precipitation. Interestingly, for deviations from the typical ENSO-precipitation relationship (i.e., dry- vs. wet-El Niño JFMs and dry- vs. wet-La Niña JFMs), the resulting anomalies in the North Pacific as well as WHWP appear to be similar in size and magnitude. Thus, during the unexpectedly wet 1973 JFM or unexpectedly dry 1990 JFM, for example, these two SST regions may have modulated the effect of other large-scale climate variables, such as equatorial Pacific SST, on regional precipitation.

Finally, wavelet analysis is applied to the observed station-averaged JFM precipitation totals to identify different frequency signals that may exist in the dataset. More specifically, wavelet

analysis is mainly used to detect the changing of dominant periods with time. Wavelet analysis decomposes a time series into time-frequency space to identify significant modes of variability and illustrate how variability may change with time (Torrence and Compo, 1998). Using a Morlet 6.00 transform (Morlet et al., 1982) on the station-averaged JFM precipitation time series, signals at a ~3-5-year band, ~12-16-year band, and ~24-year band are identified as statistically significant at the 95% confidence level (Fig. 9).

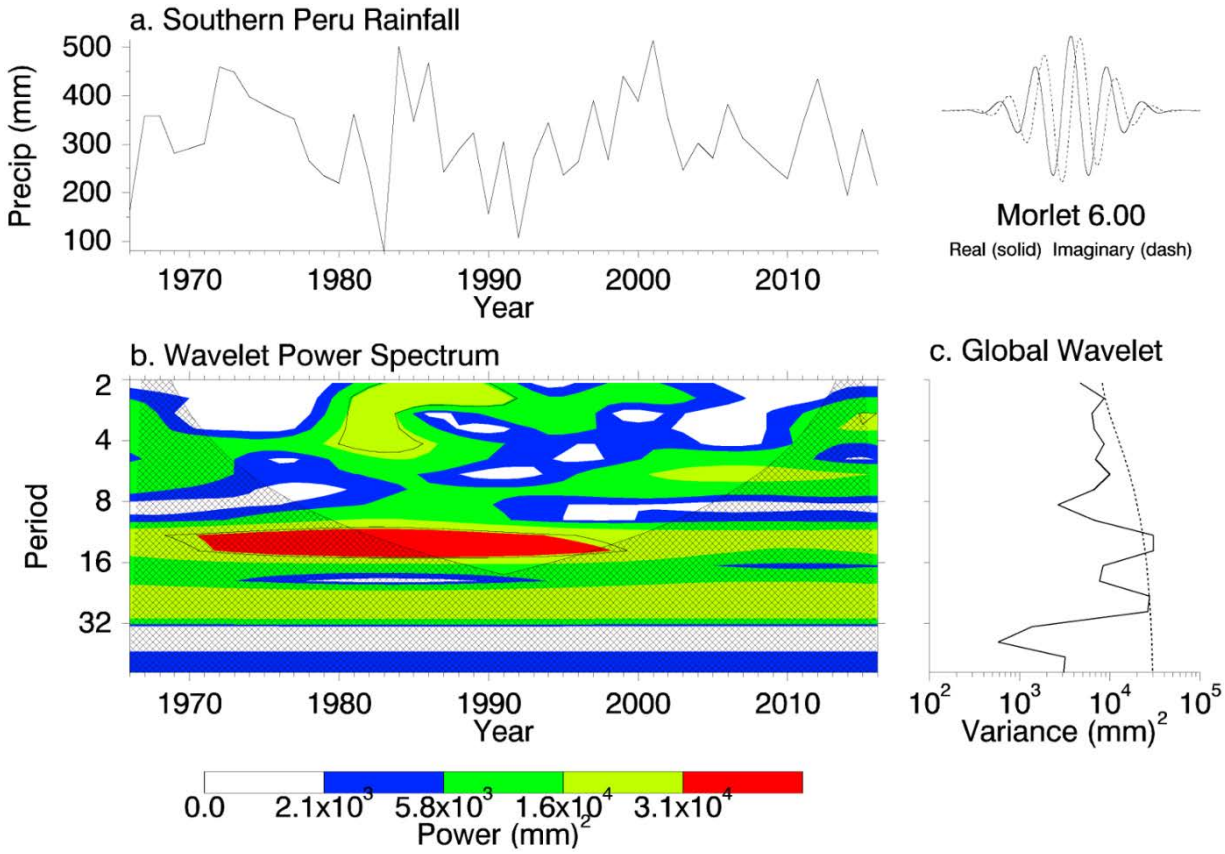

Figure 9: (a) Precipitation time series, (b) statistically significant signals at T = ~3-5, ~12-16, and ~24 years (statistically significant periods at 95% confidence level outlined), (c) global wavelet variance with 95% confidence level delineated by dotted line.

The identified signals at ~3-5 years and ~12-16 years are likely indicative of ENSO and perhaps PDO, respectively. These identified underlying periodicities of the precipitation data further affirm the inclusion of large-scale climate indices with both relatively short and long periods of oscillation. Occasionally, wavelet spectrum analysis can artificially amplify the power of longer periods. To determine whether the ~24-year signal is truly statistically significant, further testing, such as a Fourier power spectrum, may be warranted (Wu and Liu, 2005), but not undertaken here.

In total, 11 potential predictors are identified for prediction of station-averaged JFM precipitation based on previous literature and inference from spatial correlation maps, composite maps, and global wavelet analysis (Table 1). These potential predictors include both established climate indices and relevant regions of SST, SLP, and GH (as well as gradients of these variables).

All potential predictors included in the model framework display a statistically significant correlation with at least one of the first three PCs of the station-averaged precipitation time series. In addition, five potential predictors are also significantly correlated with the station-averaged times series of precipitation, and marked with asterisks in Table 1.

Table 1: The suite of potential predictors for JFM precipitation; correlations are based on JFM total precipitation and spatial averages across the regions noted, with statistically significant correlations marked with an asterisk.

Name	Large-scale climate variable	Time frame	Spatial region		Corr. w/ JFM precip.	Most Correlated PC (r)
Niño 3.4	SST	OND	5° N-5° S	170° W-120° W	-0.53*	PC1 (-0.52)
PDO	SST	OND	all areas north of 20° N		-0.19	PC2 (-0.35)
NP	SLP	D	65° N-35° N	160° E-140° W	-0.18	PC3 (0.28)
WHWP	SST	OND	28° N-8° N	110° W-40° W	-0.16	PC3 (-0.32)
	SST	OND	0° -5° S	160° W-140° W	-0.54*	PC1 (-0.54)
	SLP	D	35° N-20° N	150° W-135° W	0.15	PC2 (-0.36)
	SST gradient	OND	0° -15° S (25° S-40° S)	15° W-35° W (15° W-35° W)	0.30*	PC2 (-0.29) PC3 (0.28)
	SST gradient	OND	50° N-40° N (35° N-30° N)	150° W-135° W (180° -165° W)	0.38*	PC3 (-0.37) PC2 (0.27)
	GH 200 hPa	D	10° S-15° S	70° W-65° W	-0.35*	PC1 (-0.31)

Methods.

Statistical forecasts have been developed and evaluated for many applications globally, although more effort is still focused on the application of dynamical model predictions; however, there are numerous advantages for selecting statistical models for season-ahead precipitation prediction over other methods involving global atmospheric general circulation models (GCMs), most notably reviewed by Xu (1999). These include GCMs' inability to represent sub-grid features and

dynamics and mismatches between GCMs' strengths and hydrology needs (atmospheric vs surface), both of which statistical models can address. Dynamical models are exceptional tools for macroscale climate modeling, but can struggle at the local scale, like that of the project area. Additionally, the complex topography of the region complicates the use of GCMs for regional predictions. For this case, the merits of statistical models appear to outweigh those of dynamical modes.

Methods: Principal Component Regression-based Prediction Model.

A PCA coupled with a multiple-linear regression model construct, otherwise known as PCR, is used to predict station-averaged JFM seasonal precipitation for the study region. In this case, the method used to develop the model is advantageous because it accounts for the multi-collinearity present among several of the identified potential predictors (von Storch and Zweirs, 2001) and standardizes all resulting PC values so as not to cause any unintentional preference. After a PCA is performed on the set of area mean values of the identified potential predictors, the PCs are fit to a multiple-linear regression, given as:

$$y = \beta_0 + \beta_1 x_1 + \cdots + \beta_n x_n + e \quad (1)$$

where y is the observed JFM total precipitation, β_0 is a constant, $\beta_1 \ldots \beta_n$ are coefficients, $x_1 \ldots x_n$ are the PCs, and e is the error term. Coefficients are determined using the ordinary least squares method (Helsel and Hirsch, 2002).

To create a parsimonious model and minimize overfitting, the optimal number of PCs (i.e. predictors) is selected using the generalized cross-validation (GCV) skill score (Walpole et al., 2012; Block and Rajagopalan, 2007), given as:

$$GCV = \frac{\sum_{t=1}^{N} \frac{{e_t}^2}{N}}{(1-\frac{m}{N})^2} \quad (2)$$

where N is the number of data points (JFM seasons in the study), e_t is the prediction error or residual (the difference between model predictions and observations), and m is the number of PCs retained as predictors. GCV scores are computed for each model iteration (models with varying numbers of PCs retained), with the preferred model having the lowest GCV score. Models that overfit may have smaller prediction errors, but are penalized for having a larger number of predictors.

After selecting the optimal number of PCs to incorporate into the model, a drop-one cross validation prediction framework is applied to the 51 years of available data. The cross-validated predictions are assembled into a hindcast for the entire period of interest. This includes – for each year of the hindcast – dropping the predictor data (Z) from the year being hindcasted, forming new PCs (and EOFs) conditioned on the remaining years, and fit to observations using multiple regression, providing an intercept coefficient, regression coefficients, and error term (Stone, 1978). The predictor data (Z) from the year dropped are then projected onto the EOFs to provide PCs for the dropped year. Finally, these PCs are multiplied by the appropriate regression coefficients and added to the intercept coefficient to provide a deterministic precipitation prediction for the dropped year. This is repeated for each year.

To create ensemble hindcasts, error terms from all years are assembled and a distribution is fit (using a kernel density estimator; the distribution is approximately Gaussian). For each hindcast year, 1,000 random draws from the distribution are added to the deterministic precipitation prediction to form an ensemble.

Methods: Extended Lead Time of Predictions.

In the initial version of the model, predictors are drawn from OND, such that predictions may be issued on January 1st for JFM precipitation. This information may be too late, however, for certain stakeholders (e.g. farmers) who have already made critical decisions regarding their operations and short- to mid-term output goals. Extending the prediction lead time is explored by evaluating progressively earlier 3-month periods. For example, shifting the predictor season to SON, a JFM precipitation prediction would instead be issued on December 1st. The potential predictors for each lead time analyzed are identified in similar fashion to that of the OND predictor season model.

Methods: Spatial Disaggregation of Predictions.

Although seasonal predictions of station-averaged regional precipitation may benefit planning at a larger scale, such as by regional water councils or federal entities, more localized predictions of precipitation may prove to be advantageous for sectoral decision-making (mining, farming, etc.). To address this, spatial disaggregation of predictions from the regional-level to the station-level is evaluated. Using the regional-level categorical prediction probabilities for each year (above normal, near normal, and below normal; Fig. 10), ensemble predictions for each station are generated based on that station's own climatology. For example, the categorical probabilities at

the regional-level for 2016 are predicted as 2% above normal, 7% near normal, and 91% below normal. For each station, JFM precipitation observations from all other years (excluding 2016) are randomly selected 1,000 times from that station's JFM precipitation distribution conditioned on the regional probabilities. Thus, the ensemble of predictions for that station for 2016 will have approximately 91% of its members from the below normal category, 7% near normal, and 2% above normal.

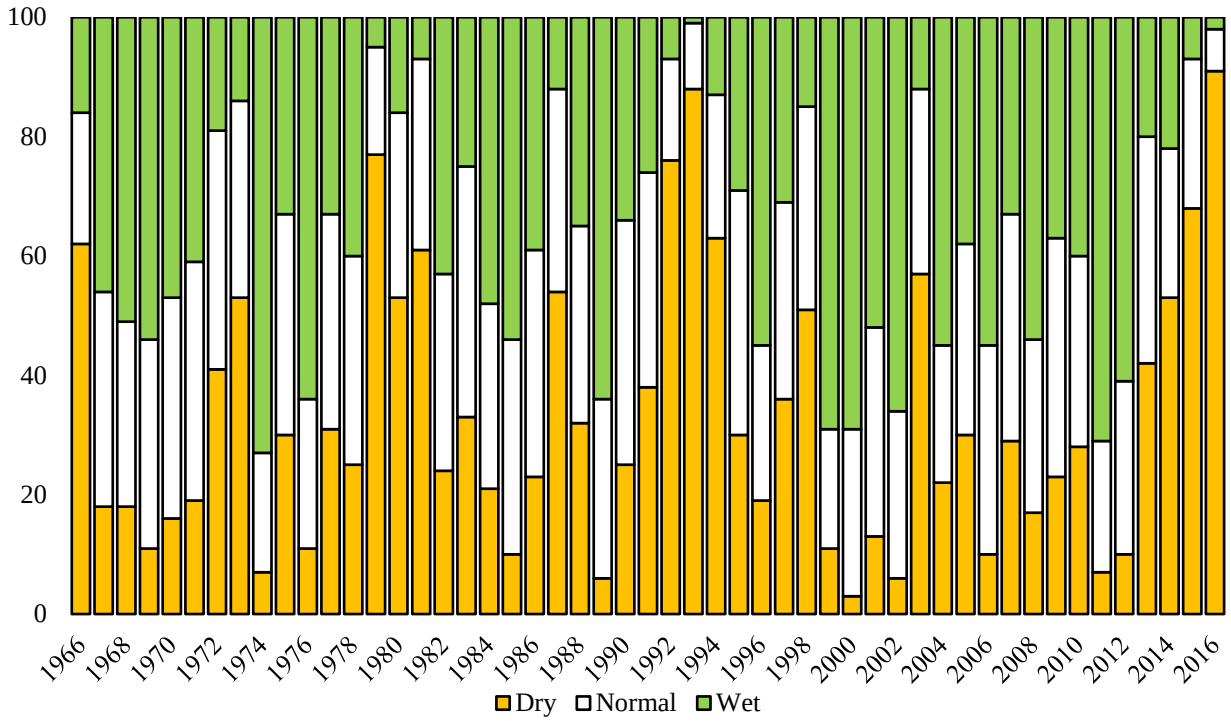

Figure 10: Categorical probabilities for JFM precipitation totals (y-axis) in each year, as predicted by the regional-scale model.

The purpose of spatially disaggregating in this fashion is to maintain the statistical integrity of the regional-level prediction while reflecting appropriate magnitudes of precipitation experienced at each station. This methodology ensures that regional- and station-level categorical prediction probabilities match even though absolute precipitation magnitudes across stations may vary significantly (Maraun, 2013). Essentially, the probabilities at the regional-level are used to generate a best estimate of absolute precipitation amounts at the station-level. Because the regional and station predictions are related, a dependent t-test for paired samples is applied to test for significant changes or differences between these two. A dependent t-test result of no statistically significant change is desired.

Methods: Wet/dry Day Frequency Analysis.

Although predictions of JFM seasonal precipitation totals may be useful for a variety of stakeholders throughout the region, some may prefer additional detailed information such as the frequency of precipitation events expected across a given rainy season. The number of wet or dry days and the intensity of precipitation events can have widespread and serious agronomic/phenologic (Robertson et al., 2008) and infiltration/runoff (Mandal and Nandi, 2017) implications. Such information may also be informative to condition stochastic weather simulators for a wide range of hydrologic or agricultural models (Robertson et al., 2006). To evaluate seasonal statistics of wet/dry day frequency for southern Peru, six of the 29 stations having readily accessible daily data are analyzed. Analogous to the seasonal total precipitation prediction modeling approach, spatial correlation mapping, composite mapping, and global wavelet analysis are all utilized to identify potential predictors describing the expected number of wet days across the JFM season.

Methods: Model Evaluation.

The cross-validated ensemble hindcasts and ancillary applications of the model are evaluated deterministically and categorically in this study using three metrics: Pearson's correlation coefficient between observed values and the median of the ensemble forecast; rank probability skill score (RPSS); and a hit-miss statistic presented as contingency tables.

RPSS is based on the ranked probability score (RPS), which measures the categorical accuracy of forecasts (Wilks, 2011). For this study, categories are based on three equal terciles from the observed record (e.g. splitting the ordered observed record into three categories with 17 years in each), and represent above normal (greater than 350 mm), near normal, and below normal (less than 270 mm) total seasonal precipitation. RPS is the cumulative squared difference between categorical probabilities for forecasted and observed conditions, and takes the form:

$$RPS = \frac{1}{K-1}\sum_{m=1}^{K}[(\sum_{k=1}^{m} f_k) - (\sum_{k=1}^{m} o_k)]^2 \quad (3)$$

where K is the number of categories, f_k is the predicted probability for the k^{th} category, and o_k is the observed probability for the k^{th} category (1 if the observation falls in that category and 0 if not). RPS ranges from 0-1, with a perfect forecast scoring 0. RPSS provides the relative improvement

of a prediction as compared to a reference prediction – typically climatology (distribution of long-term historical observations), and is given as:

$$RPSS = 1 - \frac{RPS_{forecast}}{RPS_{climatology}} \quad (4)$$

An RPSS value less than zero indicates no forecast skill over the reference climatology forecast (i.e. the forecast model does not outperform climatology). Values greater than zero represent a skillful forecast. A value of one represents a perfect categorical forecast.

The hit-miss statistic describes the occurrence of median model predictions falling into the observed category (above normal, near normal, or below normal conditions). Results are presented in a three-by-three matrix, or contingency table, that illustrates the performance of the model for each category. Contingency tables are an alternative method of assessing the precision of model predictions that relies on categorical probabilities as opposed to simpler methods such as correlation (Svensson, 2016). Of particular interest in this study is the hit rate statistic, or the percentage of time the model accurately predicts (categorically) the actual observed condition, as well as the double miss rate statistic, or the percentage of time the model makes a two-category error. Because prediction of regional meteorological drought is of particular interest, the likelihood of extremely dry conditions is also considered. For this case, extremely dry conditions are defined as station-averaged JFM precipitation less than 250 mm, which occurs approximately 25% of the time, or during 13 years across the time series.

Results.

Results: Principal Component Regression-based Prediction Model.

The best performing model, as determined by GCV, includes the first four PCs explaining 83% of the variance in the original potential predictors. The median of the cross-validated, ensemble predictions of JFM precipitation (Fig. 11) correlates with observations at r=0.58.

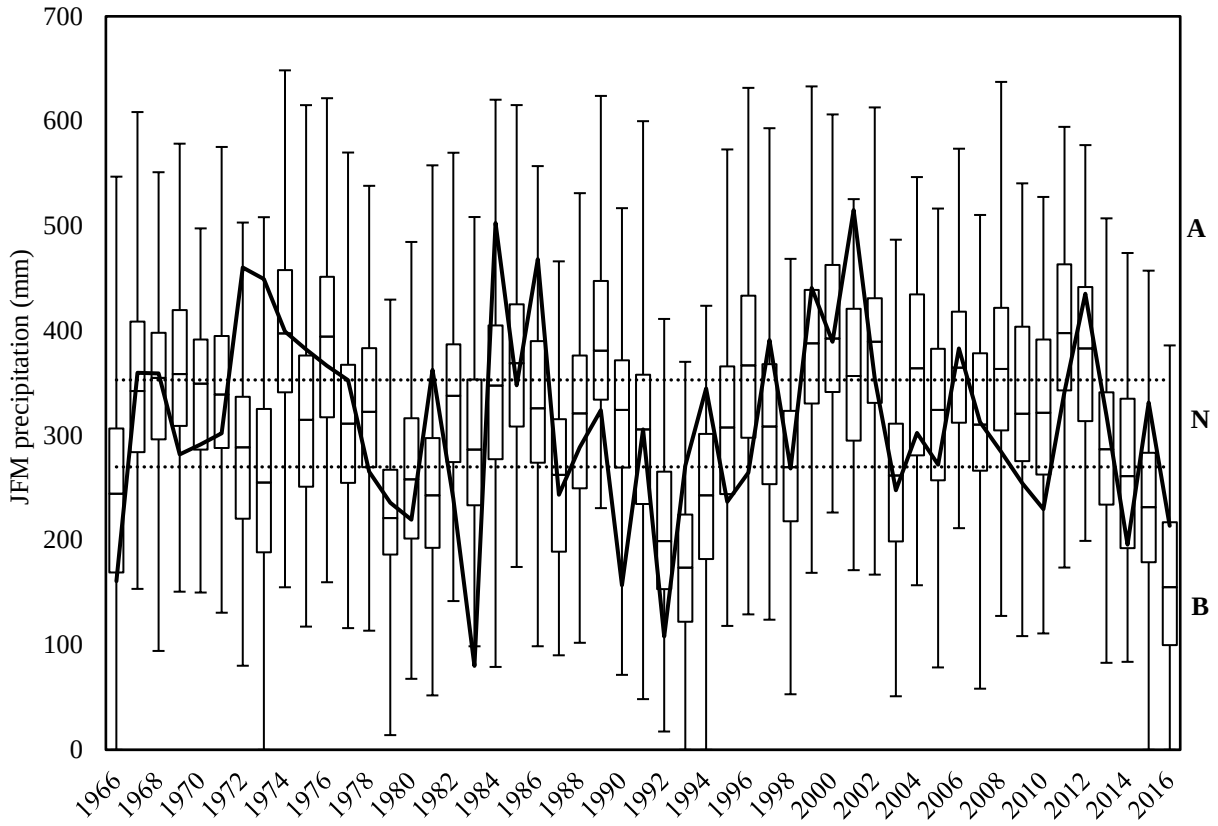

Figure 11: Box plots of cross-validated, ensemble forecasts of JFM precipitation with observed conditions (solid black line) and categorical thresholds (dotted lines, with delineated categories labelled A, N, and B) included.

The median RPSS score for the model is 0.16, indicating marginal, yet noteworthy, improvement over climatology. The model also scores a hit rate of 51%, predicting the correct category in 26 of 51 years (Table 2). With specific regard to below normal conditions, the PCR prediction has a 59% hit rate, with 10 of 17 instances correctly predicted.

Table 2: Hit-miss matrix with three equal categories: above normal (A), near normal (N), and below normal (B) precipitation.

		Predicted conditions		
		A	N	B
Observed conditions	A	**5**	9	3
	N	2	**11**	4
	B	0	7	**10**

Above normal (A), near normal (N), below normal (B)

For the 49% of years in which the model missed the observed category, only three times did the model miss by two categories. In all three cases, below normal conditions are predicted yet above normal precipitation is observed (similar to what occurred in 1973). Overall, though, the model has a strong tendency to predict near normal conditions too often (53% of the time versus an expected 33%). It is apparent that the weakest categorical performance is in predicting above normal conditions, with a hit rate of only 29% (viz., 5 predicted out of 17 actual wet seasons).

Since drought prediction is of particular interest in this study, an alternative hit-miss metric that uses only two categories – extreme below normal conditions (eB) and above normal/near normal conditions (A/N) – is also evaluated. Here, extreme dry conditions are defined as the lowest quartile of JFMs on record (specifically, 13 years with less than 250 mm of JFM precipitation). The alternative hit-miss metric has a hit rate of 80% in general and accurately predicts 62% of eB conditions (Table 3), a notable improvement compared with the tercile-based hit-miss metric.

Table 3: Hit-miss matrix with only two categories: above normal/near normal (A/N), and extreme below normal (eB) precipitation.

		Predicted conditions	
		A/N	eB
Observed conditions	A/N	**33**	5
	eB	5	**8**

Above normal/near normal (A/N), extreme below normal (eB)

Overall, model predictions demonstrate moderate skill improvement over predictions conditioned solely on climatology as well as one conditioned on an ENSO index. While a simple linear regression model using OND Niño 3.4 as a sole predictor for JFM precipitation correlates at r=0.53 (only 0.05 less than the more complex PCR model), the RPSS of this Niño 3.4 model is -0.38, or inferior to climatology.

Comparing hit-miss metrics, both models perform similarly for tercile-based categories; however, the Niño 3.4 model does not exhibit as much improvement for the two-category assessment (predicting only 23% of eB years correctly). Both models fail to accurately predict 1973

(unexpectedly wet) and 1990 (unexpectedly dry); however, the PCR model does accurately predict JFM 2014 as dry, even though neutral/weak La Niña conditions existed prior.

To understand the importance of equatorial Pacific SSTs, a second hindcast model is developed using only 9 of the 11 original potential predictors, with Niño 3.4 and SST from 160° W-140° W 0° -5° S dropped. Using the same cross-validated PCR methodology (as well as GCV to determine the optimal number of potential predictor PCs to incorporate, i.e., 3), deterministic hindcasts for the period of record are produced (Fig. 12).

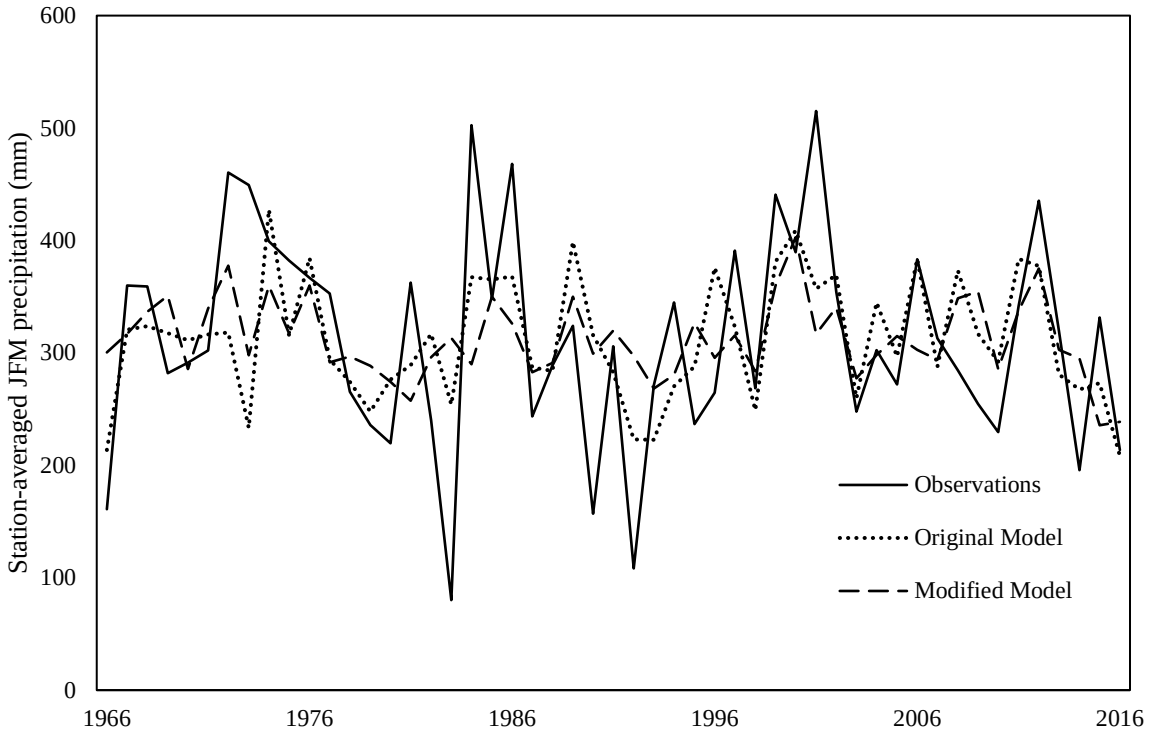

Figure 12: Observed conditions for the period of record, as well as hindcasts produced using the original model (11 potential predictors, 4 PCs) and the modified model (9 potential predictors, 3 PCs).

When comparing the results of the modified model to the original model, the importance of including ENSO in a model construct for precipitation prediction in southern Peru is highlighted. For example, the correlation coefficient between predicted conditions and observations drops from r=0.58 to r=0.37 for the original and modified models, respectively (skill reduced by roughly one-third). In addition, RPSS drops to only 0.05% from the original 16%, indicating that the

information provided by the modified model is just barely more skillful than climatology. The hit-miss metric also illustrates the diminished skill of the modified model (Table 4).

Table 4: Hit-miss matrix for the modified model with three equal categories: above normal (A), near normal (N), and below normal (B) precipitation.

		Predicted conditions		
		A	N	B
Observed conditions	A	**6**	10	1
	N	0	**15**	2
	B	1	14	**1**

Above normal (A), near normal (N), below normal (B)

The modified model displays an evident bias towards predicting near normal conditions (more than 75% of the time). While the hit score of this model is reduced to 43%, more striking is the fact that the modified model produces an instance in which above normal conditions are prognosticated, but below normal conditions are experienced – perhaps a more devastating outcome for this region than a situation with below normal predictions but above normal observations). These metrics reflect the critical importance of including ENSO in regional precipitation prediction.

Results: Extended Lead Time of Predictions.

For longer leads, no additional predictors were identified as statistically significant for inclusion into the model. In fact, the correlation between JFM precipitation and predictors typically weakened slightly with increased lead time; however, predictions created using potential predictors from extended lead times of SON and ASO are still skillful. Correlations between predicted and observed JFM precipitation only drop slightly (Fig. 13). RPSS also remains positive through ASO.

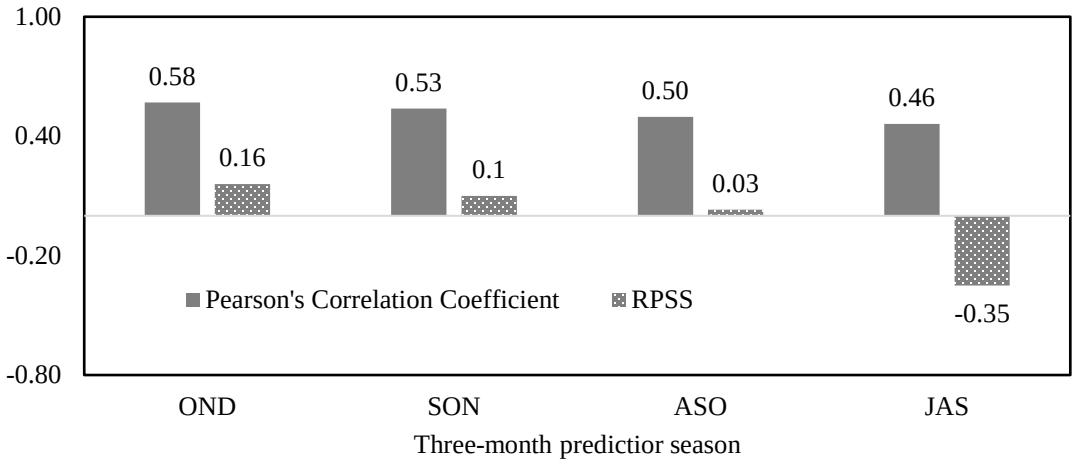

Figure 13: Correlation coefficients between observed and modeled JFM precipitation and ensemble RPSS for various lead times.

Upon using the three-month predictor season of JAS, however, RPSS drops below 0, indicating that predictions produced using JAS climate information (and issued on October 1), would have less skill than those produced using simple climatology.

Results: Spatial Disaggregation of Predictions.

None of the stations experience statistically significant decreases in correlation as a result of spatial disaggregation. For two of the stations, correlation values between station-level predictions and station-level observations increase (statistically significant at the 95% confidence interval) as compared with correlation values between regional-level predictions and station-level observations. (It should be noted that there is a 5% probability that this happens by chance). The remaining stations exhibit no statistically significant change in correlation as a result of station-level scaling. Five of the stations have significantly improved RPSS values while only one of the stations has a new RPSS value lower than zero. As expected, given identical categorical prediction probabilities, station-level hit scores are nearly identical to regional-level scores (51% overall accuracy), with more accuracy in predicting near normal and below normal conditions.

Results: Wet/dry Day Frequency Analysis.

Interestingly, the first PC of the data captured approximately 85% of the variance in the number of wet days for all six stations with daily data. High correlations are observed between this first PC and SST within the region typically associated with ENSO. No additional regions or climate

variables (e.g. sea level pressure, geopotential height, etc.) are identified using this method. Further, composite mapping and global wavelet analysis yield no additional potential predictors for incorporation into the prediction model. Thus, the wet/day frequency model uses only the OND Niño 3.4 season-ahead index as a direct predictor of wet days in any given JFM season. Using the same cross-validation method already described, the number of wet days per season is predicted for each station.

In addition to correlation coefficients between the predicted and observed number of wet days, the average prediction error for above-average and below-average years is reported for each station. Station-specific statistics are listed in Table 5.

Table 5: Correlation values and average absolute errors for predictions of wet days at each station.

Station (average number of wet days)	Correlation value (r) between prediction and observation	Average absolute error in years with above average number of wet days	Average absolute error in years with below average number of wet days
1 (25 days)	-0.50	10 days	9 days
2 (36 days)	-0.53	11 days	9 days
3 (51 days)	-0.48	11 days	10 days
4 (54 days)	-0.39	12 days	12 days
5 (54 days)	-0.53	8 days	9 days
6 (33 days)	-0.59	10 days	9 days

Correlations between predictions and observations range from r=-0.39 to r=-0.59, with the model performing slightly better in predicting the number of wet days in drier years. In general, however, the simple linear model displays an average absolute error ranging between 8 and 12 days.

To consider overall model performance, a hit miss metric quantifies skill in the two previously introduced categories of years (Table 6) – years with above average number of wet days (W) and years with below average number of wet days (D).

Table 6: Hit miss metric for model predictions of years with above and below average numbers of wet days.

		Predicted conditions	
		W	D
Observed conditions	W	**105**	41
	D	43	**103**

Above average number of wet days (W) and below average number of wet days (D)

Overall, the model correctly predicts whether JFM will have an above or below average number of wet days with an accuracy of ~72%. The model, however, has a notable bias towards over-predicting near normal conditions (Fig. 14).

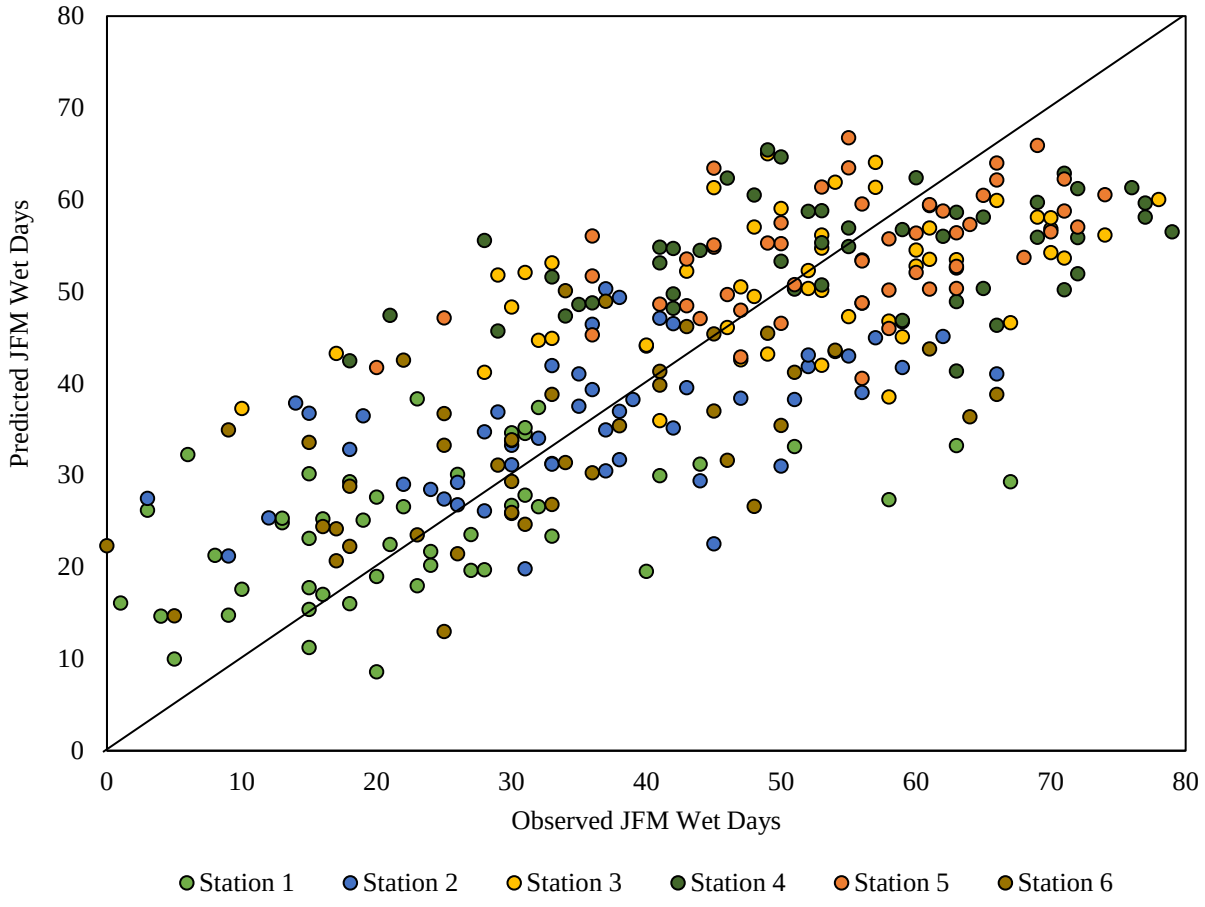

Figure 14: Observed versus predicted number of JFM wet days for six stations across 1966-2016.

CHAPTER 3: ENSO INDEX-BASED INSURANCE FRAMEWORK

Data Description.

Departmental crop data are collected by the Office of Economic and Statistical Studies (in Spanish, Oficina de Estudios Económicos y Estadísticos, or OEEE) within the Ministry of Agriculture and Irrigation (in Spanish, Ministerio de Agricultura y Reigo, or MINAGRI). OEEE maintains a rich collection of production, area, yield (production per area), and commodity prices for hundreds of crops, in some cases spanning all the way back to 1950. For the four departments in question, a total of 42 major crops are considered for candidacy. In general, the dataset tells a story of increasing yields across time, with highly variable and relatively low yields in the early years, increasing and stabilizing over time. All crop yield data are linearly detrended to account for technological and management improvements.

The monthly precipitation data used in Chapter 2 of this thesis is also used in this chapter. Similarly, ENSO indices evaluated for incorporation into the insurance framework are taken from NOAA ESRL-PSD and are publicly available.

Index-based Insurance as a Solution.

In general, farmers of the region do not have access to crop insurance products because administrative capacity to implement such a product is limited. This has been the case since at least 1998 in the aftermath of that year's El Niño induced drought, when some flurries to create a multi-peril crop insurance for the region were met with hesitation from the reinsurance community and international entities (Mahul and Stutley, 2009). The few products that were designed in coordination with certain private entities eventually lost traction amongst stakeholders and were fully dissolved after 1999. National companies faced further challenges in southern Peru relating to low levels of penetration into the market because of the scattered and diverse population of the region and in certain cases the nature of informal farming operations (Vera, 2006). While one agricultural insurance product is currently offered by the Peruvian company La Positiva Seguros on a nationwide basis against catastrophic losses (Peña Henderson, 2016), only 8% of farmers in southern Peru have adequate credit to acquire such a product (Robles, 2015).

Although agriculture insurance has been slow to develop in southern Peru in the recent past, the national outlook as of recent has been one of enthusiastic development and exploration of new

insurance products. The Peruvian national government passed Ley Nº 28939 in 2006 (Ley Nº 28939, 2006) as a legislation to support national agricultural and irrigation interests. Among other action items, the law allocated the equivalent of $14 million USD to the development of crop insurance programs. One approach recently explored is index-based insurance, a relatively new but innovative concept developed as an alternative to traditional crop insurance frameworks (Hansen et al., 2007; Hellmuth et al., 2009). Index-based insurance uses a measurable variable, such as temperature, precipitation, wind, etc., as an indicator of the magnitude of losses that likely occurred for policyholders in any given growing season (Miranda and Farrin, 2012).

In addition to reducing administrative costs and providing timely payouts, index-based insurance also minimizes moral hazard (i.e., a farmer purposefully letting their crop fail for a payout) and adverse selection (i.e., a farmer using information unfairly to their advantage in deciding whether or not to purchase insurance) (Luo et al., 1994; Dick and Stoppa, 2011). These benefits of index-based insurance are accompanied by some disadvantages, the most challenging being basis risk, when a farmer's insured loss does not correlate with the indicated index payout. There are also serious concerns regarding the societal aspects of these frameworks, such as communities' willingness to participate in index-based insurance programs and exactly how funds are distributed in certain social contexts. Other typical disadvantages associated with index-based insurance, such as the need for high quality and extensive datasets as well as enabling policy environments, are currently non-issues in Peru (Chiock Chang, 2016; Ley Nº 28939, 2006).

The utility of index-based insurance products has been demonstrated previously (Barnett and Mahul, 2007; Barrett et al., 2007), with numerous Peru-specific examples illustrating the potential to transfer risk from those most vulnerable. Some of these experiences include, but are not limited to: behavioral economic experiments involving area-yield index insurance for cotton in Ica that produced evidence that insurance may help reduce the fear of losing collateral that prevents potential borrowers from taking loans (Galarza, 2009); crop weather index insurance in Piura relating to the impact of flooding on harvests and the potential posed by micro-lending schemes in mitigating these impacts (Skees et al., 2007); and an ENSO-based index insurance product against floods in northern Peru that demonstrated the skillfulness of ENSO indices in determining payouts in the aftermath of floods (Khalil et al., 2007). Furthermore, Red Cross Red Crescent of Peru has recently investigated the potential for forecast-based financing, coupling index-based insurance

and index prediction, in the specific context of cold temperature and snow events in the mountains, river flooding in the north, and other ENSO-related weather events along the coast. While the policy environment which enabled these success stories still exists, the potential for an index-based insurance product or forecast-based financing framework has yet to be exploited in southern Peru for protection against drought.

Selection of an Index and Candidate Crop.

Seasonal precipitation plays an integral role in the agricultural operations of a majority of farmers in the region. While the rainy season may last anywhere from early-November to late-April depending on the year, the main season of interest for this study is JFM. During this season, some locations receive up to 85% of their annual precipitation as determined by analyzing precipitation data from the 29 gaging stations scattered throughout the region.

While it is evident that several large-scale climate mechanisms influence the region's hydrologic cycle (Mortensen et al., 2017; Wu et al., 2017), ENSO plays a significant role in modulating regional precipitation during these three months (Lagos et al., 2008). The generally accepted relationship is that an El Niño (a La Niña) event produces drier (wetter) than normal conditions (Vuille et al., 2000; Garreaud et al., 2003; Espinoza Villar et al., 2009; Lavardo-Casimiro et al., 2013; Cid-Serrano et al., 2015). ENSO thus serves as a potential proxy for precipitation in southern Peru, with several ENSO indices to choose from, including Niño 1+2, Niño 3, Niño 4, Niño 3.4, MEI, ONI, etc. (Trenberth, 2016), and may serve as a useful trigger for coverage. All of these indices are based on sea surface temperature anomalies (and in some cases other large-scale climate variables such as sea level pressure) in the equatorial Pacific. Because of this, these ENSO indices are considered tamper-proof.

To determine which ENSO index serves as the best proxy for regional precipitation, correlations are calculated between a concurrent index and regionally (as well as departmentally) station-averaged precipitation. Although all indices correlate well (and significantly) with precipitation, Niño 3.4 displays the highest correlations in all instances, with JFM regionally station-averaged precipitation and JFM Niño 3.4 correlating at $r = -0.575$ (Arequipa station-averaged $r = -0.535$, Moquegua station-averaged $r = -0.509$, Puno station-averaged $r = -0.533$, Tacna station-averaged $r = -0.517$). Thus, Niño 3.4 is selected as the proxy precipitation index for this study.

While many crops may be insured under such insurance products proposed here, a single crop is selected for demonstration purposes using the following: (1) a strong relationship between crop yield and interannual precipitation, (2) a strong relationship between crop yield and the Niño 3.4 index, and (3) literature documenting the crop as water sensitive and predominantly managed in rain-fed conditions. Additional factors such as societal prevalence and relevance are also implicitly considered in the process of selection.

Several crops show potential across the region (e.g., alfalfa and sweet potatoes in Arequipa; onions in Moquegua; peas and onions in Tacna; alfalfa, peas, quinoa, mashua, and lupin in Puno) with regard to the stated criteria. Ultimately production of O. tuberosa, or oca, in Puno is selected. Oca is a tuber cultivated in the High Andes and Altiplano regions of southern Peru. Interestingly, oca has been a part of the lives of people in the region for hundreds of years, even in the pre-Columbian era (Fortaleza, 2012).

Although observations of oca yields only extend from 1977 to 2014, oca illustrates lower yields during times of below normal precipitation (1983, 1993, 1997; Fig. 15), correlates with Niño 3.4 at a statistically significant level (r = 0.51), and is noted by academic literature (Alandia, 1967; Glicero, 2010) and the Food and Agriculture Organization (Valdivieso, 2010) as being highly dependent on water and vulnerable to water stress.

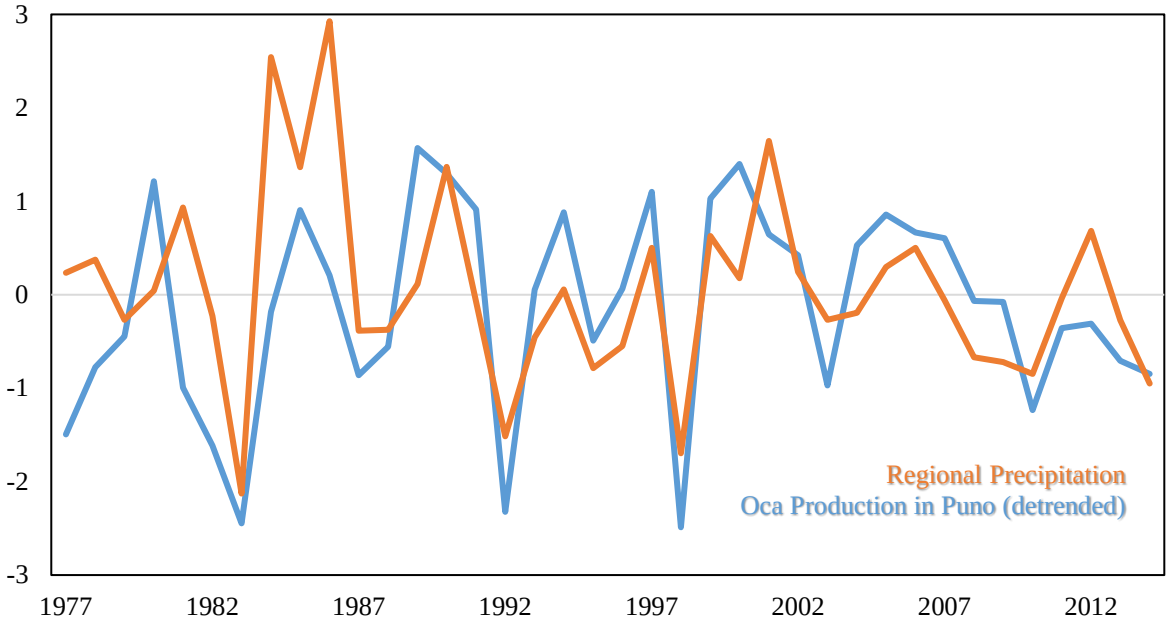

Figure 15: Normalized Puno JFM precipitation and annual oca production (1977-2014).

Methods.

Realistically, different insurance products should be developed for each individual crop at the smallest spatial scale feasible to account for the heterogeneity of precipitation and associated losses in a region (Choudhury et al., 2016; World Bank Group, 2005). To reduce basis risk further, the addition of another index, such as observed soil moisture or precipitation, could be considered. In this case, the coverage scheme would be a dual-trigger system and may allow for additional losses caused by drought to be covered. In the oca demonstration presented here, a second index that is triggered for historical years with significant losses but having ENSO neutral conditions would be advantageous. A potential multi-index framework, however, is not explore in this thesis.

While the government of Peru has been moving towards creation of insurance programs in several applications, its resources to do so are still considerably limited (Urby et al., 2010). The reinsurance community has been slow to act in Peru, partially due to the impacts of the 1997 El Niño event and subsequent 1998 drought (Skees and Collier, 2010). This reality is incorporated into product design by assuming that the program is self-insured, meaning that the product would be fully supported by the entity providing it, i.e. the government of Peru, and self-sustaining after the product's launch. Ideally multiple insurance products may be coupled that pay out at different times to hedge payouts in any given year (Bonnafous et al., 2017); however a spatially diverse premium program may also be warranted in some situations. Premiums are relative to an expected, long-term average percentage of farmers' yields, up to 7.5%, the maximum a farmer may be realistically expected to contribute (World Bank Group, 2016).

Methods: Endowment and Coverage Optimization.

The development of a product based on this premise lends itself plainly to optimization. In this optimization problem, the objective is to minimize the initial amount of resources to be allocated to the product's endowment. The solution space is governed by the inflow and outflow of resources as described above. Specifically, the value of the endowment in any given time period is equal to the value of the endowment in the prior period plus the premiums paid into the product minus the payouts of the product during that period. To simplify the problem, the premium paid into the product is assumed to be constant across time (i.e., each farmer pays the same amount every year). The premium is a relative amount (i.e., a uniformly distributed percentage of each farmer's actual yield) as opposed to an absolute value. The maximum percentage evaluated for premium payment

is 7.5%, being interpreted as the maximum as to how much, on average, a farmer could be realistically expected to contribute to a fund as a percentage of profit gained from harvest (Dick and Stoppa, 2011). Coverage, meanwhile, is a function of the selected index, Niño 3.4 in JFM, with higher payouts directly correlating with higher SST anomalies in the equatorial Pacific. Because JFM conditions are used to determine coverage, payouts would not be dispersed in this case until April 1. Depending on the case in question, the endowment is forced to be either bankruptcy adverse (i.e., endowment never dips below zero) over its full lifetime, or simply to reach the end period at a level above bankruptcy.

Although price data exists for oca, this product is initially designed with average expected yield (AEY) as a unit of measure; instead of describing the value of the endowment, premium payments, and payouts in terms of Peruvian soles or any monetary unit, the flows are described as magnitudes of expected annual average yields for oca farmers in Puno – approximately 7,100 kg/ha. With a model described in terms of yield as opposed to profit, the developed product can be applied at a variety of scales for evaluation from the regional-level (overall performance of a sector-wide product) down to the individual-scale (how one would fare if they adopted a micro self-insuring protocol). Accordingly, economic data can be applied to the derived values of the product post-development to evaluate certain financial criteria.

This assumption largely ignores the intrinsic relationship between supply, demand, and commodity price. For more exact economic insights, an additional model could be developed taking into account the price point of oca in any given year; however, this prospect is not pursued here due to the erratic nature of the Peruvian economy during the mid-1980s and early 1990s that resulted in extreme inflation rates, reaching up to over 7,000% in certain instances, which is reflected in the data and arguably unresolvable (Rojas-Suarez, 1992).

Optimization is applied to determine the coverage function for the product. The objective here is to minimize the amount of losses incurred by farmers. Three strict constraints are placed onto the payout scheme optimization problem. First, coverage paid out is equal to zero if losses incurred are less than zero in any given year. Second, coverage paid out in any given year, when appropriate, must be greater than zero but less than or equal to either the actual experienced loss or 45% of AEY (whichever is smaller), as recommended by Dick and Stoppa (2011). Finally, to minimize basis risk, losses are covered only in years when a threshold Niño 3.4 value has been surpassed –

set such that historical years with higher Niño 3.4 values all demonstrate actual losses. The final payout scheme is linear, as opposed to a step- or piece-wise function, with payouts increasing proportionally with increasing Niño 3.4 values. Payouts could be dispersed as early as April 1.

Methods: Model Evaluation.

Thus the two critical product characteristics evaluated – besides the index and trigger – are the level of premium and associated magnitude of initial endowment. The long-term viability of a concurrent-season product is evaluated by resampling, or bootstrapping (Efron and Tibshirani, 1993; Efron, 2003), the available Niño 3.4 data (1870 to present) (Rayner et al., 2003) to create 100 new simulations, each of length 100 years. Here, concurrent products (JFM) under 3% and 7% premium rate scenarios are compared using metrics including average end of life endowment, 30-year bankruptcy rate and end of life bankruptcy rate (i.e., how many scenarios are at a level below zero at year 30 and 100, respectively), and lifetime bankruptcy rate (i.e., how many scenarios at any given time fall below zero).

To evaluate the product with differing index lead times, two temporal alternatives are considered, in lieu of concurrent JFM conditions. For the first, observed Niño 3.4 index values are incrementally shifted back, month by month, to potentially take advantage of ENSO's persistent nature. In the second, predicted JFM Niño 3.4 conditions from varying lead times are investigated. The advantage of a trigger early in time – if sufficiently correlated – could be earlier payouts, perhaps even prior to the JFM season.

Results.

The payout scheme developed protects strictly against basis risk from the viewpoint of the insurer, such that that no historical events would have inappropriately paid out (Fig. 16). Subsequently, this results in some instances in which moderate loss events are not covered by the insurance product, particularly those during near-neutral ENSO conditions. Only one historical El Niño event with crop losses would not have been covered if this product had been in place. Because the payout function is linear, a relatively larger portion of losses during moderate El Niño events are covered than during strong events.

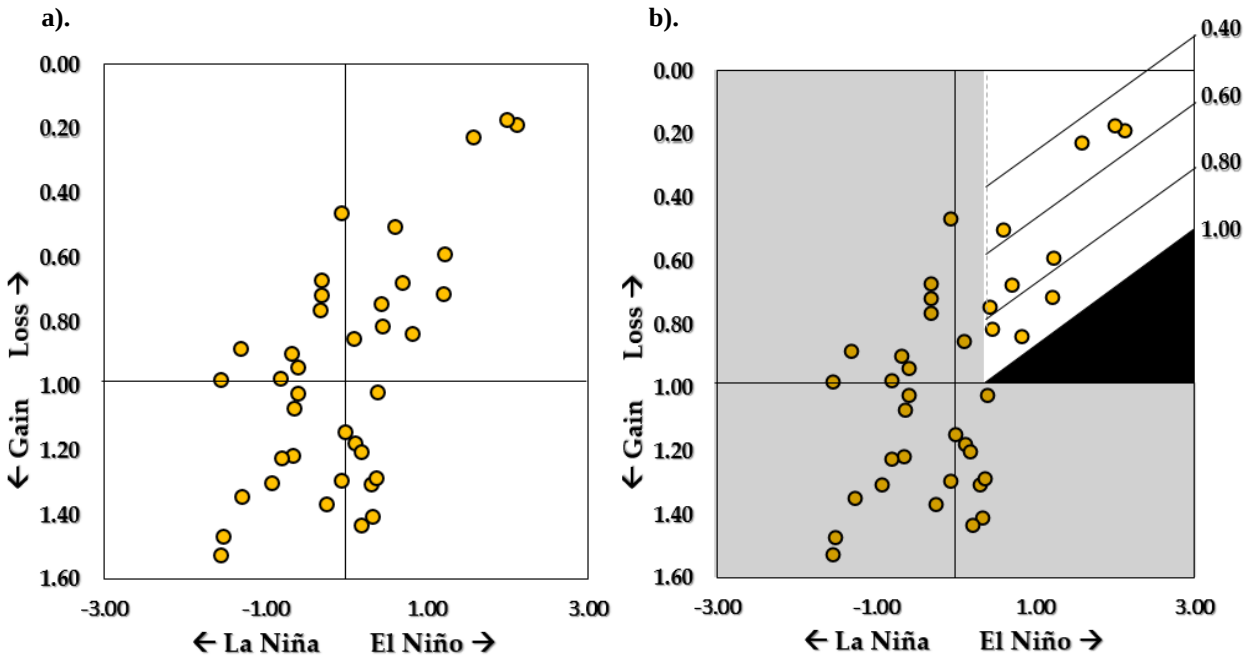

Figure 16: Developed payout scheme for insurance product. (a) Scatterplot of ENSO conditions and oca yield (in terms of AEY). (b) A graphical approximation of the proposed payout scheme. The black triangle represents the coverage provided by the product.

Using this payout scheme, the 7% and 3% premium rates are evaluated to determine the optimal initial endowment size under concurrent (JFM) conditions using historical observations (Fig. 17).

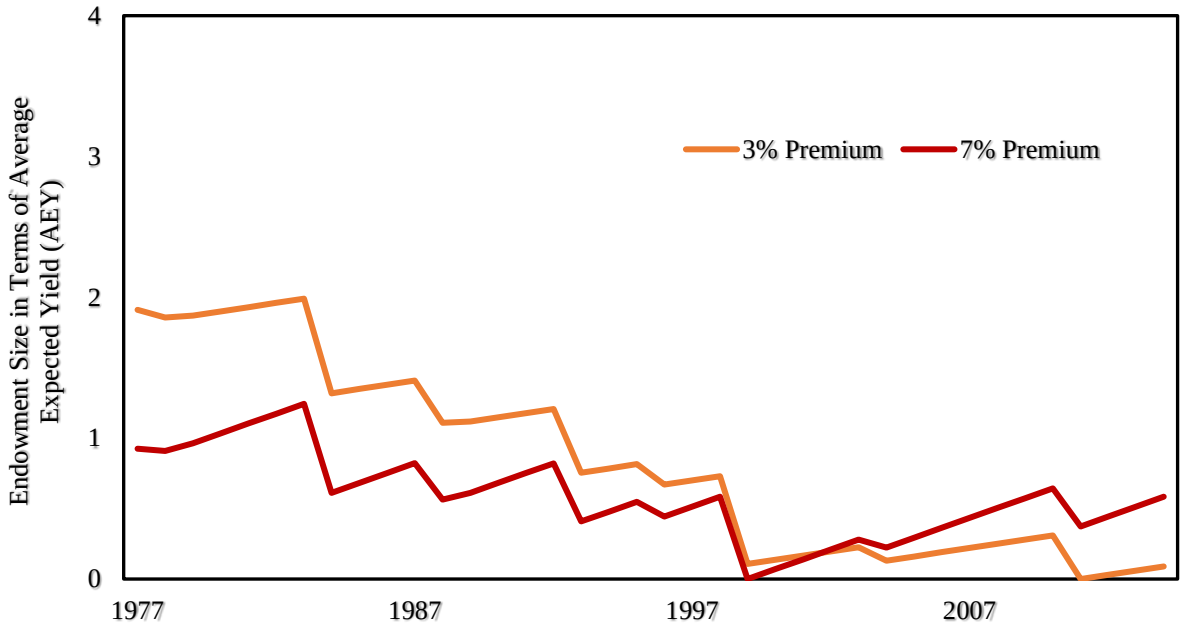

Figure 17: JFM product evaluated under 7% and 3% premium scenarios.

Products with lower premiums consistently illustrate the need for higher initial endowments. For example, an AEY of 1.8 is required for the initial endowment of a 3% premium product, while an AEY of 0.9 suffices for the 7% product. If recent economic data is applied to these figures, $2,080 and $1,040 USD per ha, respectively, would be required for the JFM product's initial endowment. This analysis was subsequently carried out for premiums ranging from 1% to 7.5% (Fig. 18).

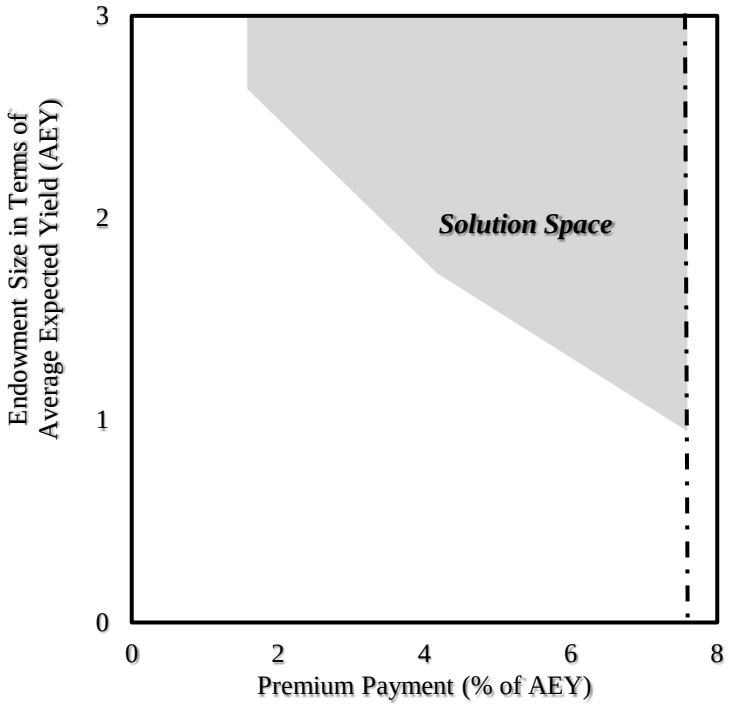

Figure 18: The required initial endowment size for various premium rates, based on 1977-2014.

Under these conditions for 1977-2014, the product never inadvertently pays out, never goes bankrupt (although does reach zero at some point by design), and never pays more than what was lost. Ten different events triggered payout for JFM losses across 1977-2014. By minimizing the initial endowment needed, a 1977-2014 hindcast reveals that products reach 2014 with only a fraction of what they possessed in 1977 (in the case of the JFM 3% premium, for example, the ending endowment fund is barely positive at 0.09 AEY).

To understand the viability of this product, the analysis may be extended to partially account for longer periods and sequencing of years not observed, using the 100 simulations of 100 years each for the 7% premium (Fig. 19) and 3% premium (Fig. 20) . The initial endowment size determined from the historical hindcast (7% = 0.9AEY and 3% = 1.8AEY) are used. Stationary conditions over the examined period are assumed.

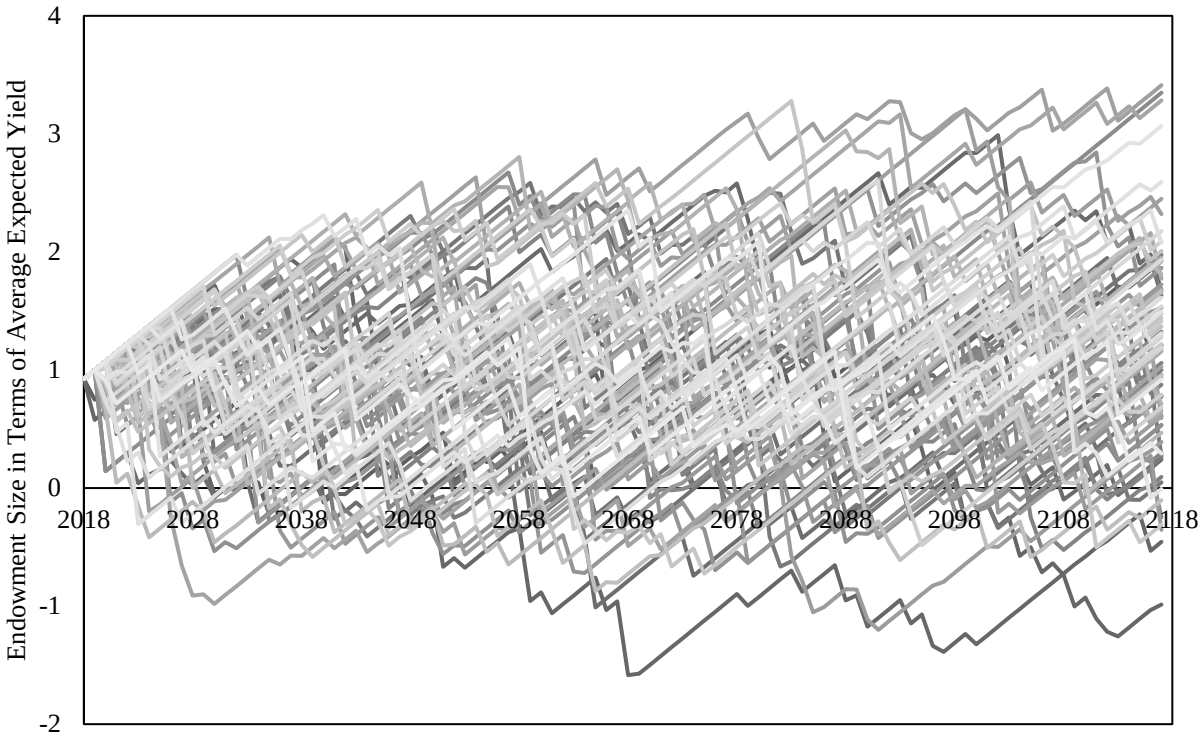

Figure 19: Size of annual endowment for 100 simulations and 7% premium; initial endowment is 0.9 AEY.

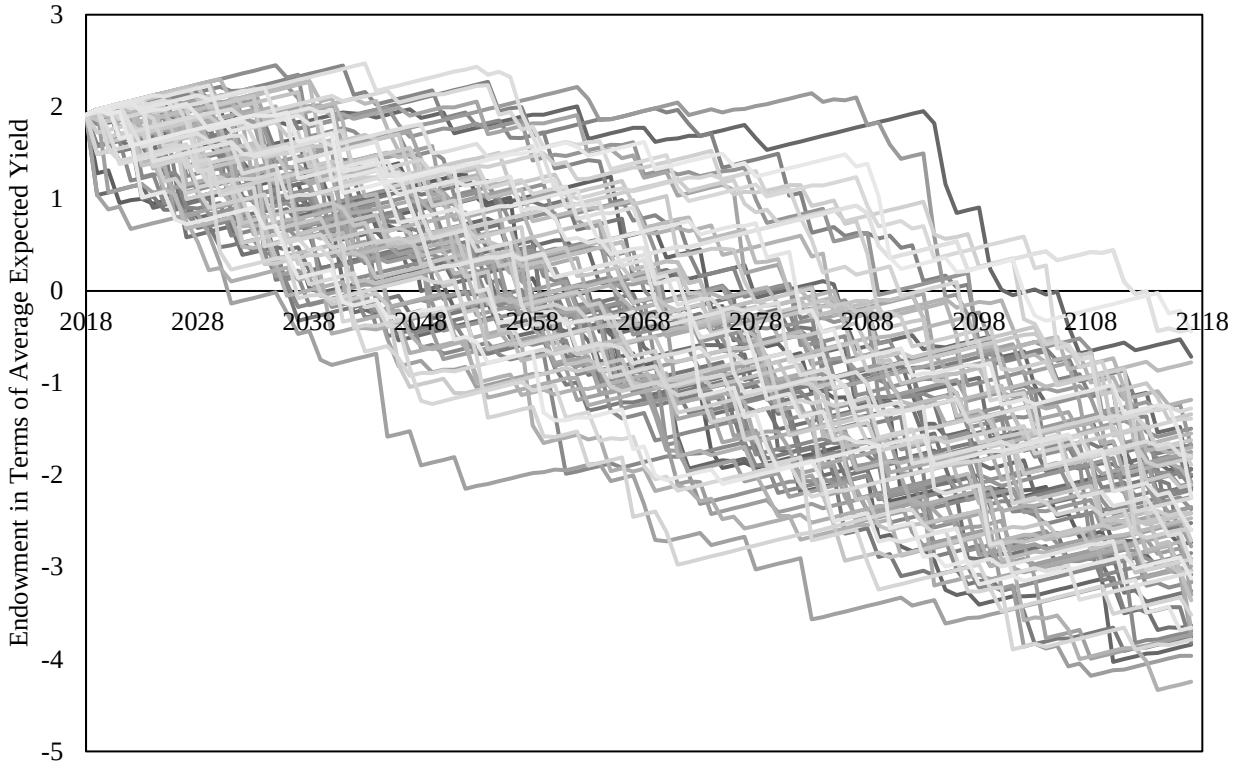

Figure 20: Size of annual endowment for 100 simulations and 3% premium; initial endowment is 1.8 AEY.

The JFM 7% premium product has an average end of life endowment of 1.19 AEY, 30-year and end of life bankruptcy rates of 14% and 9%, respectively, and a lifetime bankruptcy rate of 49%. The JFM 3% premium product has an average end of life endowment of -2.48 AEY, 30-year and end of life bankruptcy rates of 12% and 100%, respectively, and a lifetime bankruptcy rate of 100%. For both products, the range between maximum and minimum ending endowments is approximately 4.5 AEY.

Products with the Niño 3.4 index conditioned on a three-month window prior to concurrent conditions are quite similar, largely attributable to the persistent nature of ENSO. For example, using an OND Niño 3.4 index, the initial endowment values for the 7% and 3% premium products increase to 1.9 AEY ($1,920 USD per ha) and 3.27 AEY ($3,250 per ha), respectively, using the 1977-2014 period. The same ten events are covered by the OND product as by the JFM product, however, three additional years also led to payouts; that is, the Niño 3.4 conditions in OND in those three instances surpassed the threshold and would have triggered a payout, but waned by JFM and fell below the threshold (Table 7). Additionally, predictions of JFM Niño 3.4 conditions from prior seasons (developed using simple linear regression) are evaluated for the period of record for oca (Table 8).

The third and fourth columns of the tables represent the two types of basis risk that are possible in this product. In general, as the lead time is increased, the number of false coverage events remains relatively constant; however, the JAS and JJA window produce time series in which four events should have been covered, but were not. The implications of this type of basis risk are critical – in these four years of loss, farmers would not receive payouts from the product because the trigger threshold was not surpassed.

Table 7: Percent losses covered, basis risk events, and erroneous payments for product conditioned on observed Niño 3.4 values from incrementally shifted seasonal windows.

Niño 3.4 window used for product index	Percent of losses covered (compared to JFM product)	Number of false coverage events	Number of uncovered loss events	Amount erroneously paid out (as AEY)
JFM	100%	0	0	0
DJF	132%	3	0	0.19
NDJ	151%	3	0	0.36
OND	146%	3	0	0.37
SON	116%	2	0	0.28
ASO	85%	3	0	0.22
JAS	57%	2	4	0.13
JJA	45%	2	4	0.02

Table 8: Percent losses covered, basis risk events, and erroneous payments for product conditioned on predicted JFM Niño 3.4 values from incrementally shifted seasonal windows.

Niño 3.4 window used for product index	Percent of losses covered (compared to JFM product)	Number of false coverage events	Number of uncovered loss events	Amount erroneously paid out (as AEY)
JFM	100%	0	0	0
DJF	102%	3	0	0.08
NDJ	103%	2	0	0.15
OND	99%	2	0	0.18
SON	92%	2	0	0.18
ASO	80%	2	0	0.19
JAS	68%	1	3	0.17
JJA	63%	2	3	0.08

CHAPTER 4: DISCUSSION AND CONCLUDING REMARKS

Chapter 2 investigates the importance of including other large-scale climate variables (in addition to solely ENSO) in predicting regional precipitation. The developed, comprehensive model outperforms simpler models across several metrics, although the improvement is not necessarily remarkable. Additional progress could be made in the form of exploring other modeling methods as opposed to PCR. Beyond the work performed in this study, additional avenues for further research include alternative modeling approaches (i.e., LIM, temporal tendency modeling, etc.) and prediction integration into hydrology and other sectoral/decision-making models.

Model skill remains relatively constant with increasing predictor lead time, notably predictions produced using ASO predictor information for November 1. This additional lead may prove beneficial to stakeholders in the region. For example, in the 2016 drought, ANA made emergency declarations for the cities of Tacna and Arequipa at the beginning of January based on projected water availability. This allowed minimal time for city officials and local residents to prepare for the impending dry rainy season (even though exceptionally strong El Niño conditions had been predicted several months in advance by multiple entities including the National Weather Service Climate Prediction Center and Peru's Estudio Nacional del Fenómeno "El Niño"). Additionally, farmers in the region – many of whom are subsistent – had already made crucial agricultural decisions well before the beginning of the rainy season.

In addition to extended lead times, spatially disaggregated predictions could prove beneficial to several sectors impacted by spatiotemporal precipitation variability. This investigation produces disaggregated predictions with only minimal significant diminishments in skill, which may require further investigation. The governing large-scale climate mechanisms that deliver precipitation to the region more or less act uniformly across this small area of southern Peru, with relatively distinct signals, while station observations may actually be noisier in comparison.

The high correlation between number of wet days and SST in the equatorial Pacific suggests that the ENSO phenomenon not only controls the regional seasonal volume of precipitation, but also the frequency of wet days. While the prediction model of wet days achieves notable skill, the model in general displays a tendency to under-predict the number of wet days (especially in seasons in which more wet days are observed than dry). Additional prediction skill may be achievable by incorporating local variables such as antecedent soil moisture conditions or low

level winds into station-specific models, similar to disaggregation of regional precipitation predictions.

There are several limitations of the framework, including poor performance in predicting above average precipitation conditions and real-time data requirements. Although the region is highly vulnerable to drought conditions, the limited ability of the model to predict above normal conditions could translate into missed economic potential for farmers and mining operations. Improving above normal category prediction could take the form of investigating additional local variables, such as quantifying the orographic impact of the Andes and investigating other small-scale perturbations to the climate system. In general, though, the prediction framework as developed hinges on readily accessible climate data from the sources used in this study. In some cases, delayed publishing of this data may result in a delayed prediction of JFM precipitation. With some of the ancillary applications, further limitations of the framework include the regional versus local nature of predictions and associated skill and trade-offs with longer prediction lead times.

In this thesis, the statistical approach explored has produced results that are arguably more skillful than existing methods of precipitation prediction for this region of Peru. Therefore, one may be tempted to draw the conclusion that a statistical approach of this sort can be applied in a similar fashion at any other location of interest in the world (outside of southern Peru) and produce equally skillful results. A conclusion along these lines would be temerarious. Although model frameworks are transferable to other locations, there are no guarantees that one approach will still be superior to another. Furthermore, there is no guarantee that observed increases in skill in one location will translate to expected equivalent increase in skill in another location.

Chapter 3 explores what an index insurance framework might look like for oca production in Puno. In general, to reduce the risk of bankruptcy, an indirect relationship is observed between initial endowment size and required premium to be paid into the endowment.

While the concurrent 7% and 3% premium products both appear equivalently viable for certain time scales, such as 30 years, it is clear that long-term aptitude of the 7% to avoid bankruptcy is much stronger than that of the 3%. For the initial endowments assumed. That is not to say that lower premium products are inferior to those with higher premiums. Although a product with a higher premium clearly requires less initial funds from the administering party, the premiums may

prove to be too cost-prohibitive for farmers and defeat the purpose of the product. A viable insurance product must meet the goals of both the insurer and insuree.

In cases of self-insurance, e.g. a resource-strapped government, the preferred product would have as small of an initial endowment as possible, which leads to higher premiums to substantially supplement the endowment, but may also effectively price out participants. This is especially relevant for small-scale subsistence farmers in already impoverished areas of the remote Altiplano. Conversely, while a low premium may allow for a greater segment of producers to participate in the insurance program, a larger initial endowment amount would be required on the part of the government, and even then, these relatively smaller supplements to the endowment may lead to the ultimate bankruptcy of the fund over the long-term. Premiums aside, farmers are still exposed to considerable losses during neutral ENSO and La Niña events. There may be several ways to improve upon these shortcomings of cost and basis risk.

Strictly in consideration of the long-term viability of the insurance program, it would be advisable to adopt a premium policy in which policyholders would pay towards the higher end of suggested premium levels. With this range of premiums (up to 7.5%), the product as designed does not experience widespread bankruptcy during the analyzed time series. Because the product was designed in the mindset of ensuring the sustainability of the program, farmers would either have to pay potentially unbearable premiums and still be exposed to considerable losses during neutral ENSO and La Niña events, or chose not to participate in the program at all. There may be several ways to improve upon these shortcomings of cost and basis risk.

The government of Peru has allocated funds to a contingency fund for farmers in the immediate aftermath of recent drought events. While these funds serve as a version of a welfare program, the costs required to distribute such resources without prior planning could prove costly. To reduce the unforeseen high welfare costs of the current paradigm, the developed index-based insurance framework could be used as a planning tool by the government to build emergency response funds over longer periods of time. With regard to cost, it may be advantageous to draw additional funds from other governmental resources, seek private investments, or use a third-party insurer. These additional funds could serve as a supplement to bolster the initial endowment size, allowing farmers to pay lower premiums, or periodically injected to maintain solvency. Alternatively, the funds could be used to subsidize premiums to encourage farmer participation. Farmers could then

pay an additional premium if they desired expanded coverage. Both approaches result in lower contributions by farmers and expand the solution space in which the product might exist.

To reduce basis risk, the inclusion of another predictor, such as remotely sensed soil moisture or precipitation, could be considered. In this alternative, the coverage scheme would be a dual-trigger system in which if only one threshold was passed the originally developed coverage would be allocated. If both indices crossed the predefined thresholds, however, coverage could be augmented and expanded. This could allow for additional losses caused by drought to be covered. For the work undertaken in this thesis though, this potential avenue is not explored.

It is noteworthy that a product conditioned on predicted JFM Niño 3.4 conditions (as opposed to observed JFM conditions) still maintains relatively similar performance for several months prior. For oca production in Puno, a product using predicted JFM conditions based on ASO observations performs similarly to JFM observations such that farmers receive similar payouts and uncovered loss events are similar in size and frequency. If a product were to payout on November 1, as opposed to April 1, this could allow additional time to proactively manage a crop or at least prepare for reduced yields.

The time at which farmers must decide whether or not to participate in an index-based insurance program in any given year is also an important consideration. A scheme could be established such that farmers deciding to purchase insurance late or after a forecast is available may be required to pay a higher premium to receive the same level of coverage, thus addressing adverse selection.

While this product shows potential for oca farmers in Puno broadly, clearly regional production of oca are heterogeneously distributed throughout, and may require further tailoring of products to local scales. Of high relevance is the social structure under which some of these communities, especially indigenous, operate. Depending on the community, it may be necessary to provide coverage to the entire community as opposed to individual participants. In the event of a covered event, the community - and not the individual farmer - would receive the payout and then be responsible for distributing funds to those affected.

In general, index-based insurance presents a unique alternative to traditional insurance products, especially in southern Peru, where administrative capacity is low, credit is limited, and relief to past disaster has been delayed. Index-based insurance could play a large role in increasing the

resilience of communities. Because of its ability to reduce adverse selection and minimize moral hazard, index-based insurance has had success in other regions of Peru and around the world. In this case, with an enabling policy environment and a relatively rich dataset, development of a product is a tangible reality.

As illustrated with the oca demonstration, maintaining a self-insured, self-sufficient insurance product is nontrivial. Without the support of third-party entities, the design process becomes a balancing of interests between the administrator of the product and the policyholders, and risks being too cost-prohibitive and minimizing participation. An insurance product that a farmer needs but is unable to pay for is a poorly designed product. Perhaps with modification, as outlined previously, it may be possible for this product to be improved in a way such that a sustainable and affordable insurance product indeed can be achieved.

The potential posed by season-ahead precipitation prediction and index-based insurance may allow regional stakeholders more time and detailed information to proactively prepare for droughts (as opposed to reactive measures that have plagued regional drought management in the past). The lynchpin of this proactivity is effective and consistent collaboration among ANA, SENAMHI, and other public and private local, regional, and national entities. Initiatives and legislation such as the Peruvian Drought Observatory and Ley 28,939 have served as a starting point for this growth; however, the observatory currently offers minimal climate forecast information, and could benefit from the inclusion of such outputs, and the true potential of the policy environment regarding insurance implementation has yet to be fully exploited. Furthermore, a critical component of the potential benefits reaped by employing these tools is the necessity of stakeholders to understand and have faith in utilized tools, and how they relate to reality. As drought continues to deleteriously impact water supply and access in southern Peru, season-ahead predictions and index-based insurance may become more instrumental in facilitating proactive and sustainable water management in this semi-arid region of the world.

REFERENCES

Aceituno, P., and Montecinos, A.: Análisis de la estabilidad de la relación entre la Oscilación del Sur y la precipitación en América del Sur, Bulletin de l'institut Francais d'Etudes Andines, 22(1), 53-64, 1993.

Alandia, B.: "Enfermedades de la oca." Segundas Jornadas Agronomicas. 1967.

Alegría, J.F.: The Challenges of Water Resources Management in Peru, Rural Water Supply and Sanitation Project for Southern Andes of Peru, presented at IAP Water Programme Regional Workshop for the Americas in Sao Paulo, Brazil, 2006.

Autoridad Nacional de Agua – ANA: Observatorio de Sequía Peruana, UNESCO, en colaboración con Minagri, Cenepred, Indeci, y la Universidad Nacional Mayor de San Marcos, y Organización de las Naciones Unidas para la Alimentación y la Agricultura, 2014.

Autoridad Nacional de Agua – ANA: Ministerio de Agricultura y Riego ejecuta plan de contingencia por peligro inminente de déficit hídrico en el sur, artículo publicado por ANA, 2016.

Barnett, B. and Mahul, O.: "Weather Index Insurance for Agriculture and Rural Areas in Lower-Income Countries." Amer. J. Agr. Econ. 89. 2007.

Barnett, B. J., Barrett, C. B., and Skees, J. R.: Poverty traps and index-based risk transfer products. World Development, 36(10), 1766-1785, 2008.

Barrett, C. B., Barnett, B. J., Carter, M. R., Chantarat, S., Hansen, J. W., Mude, A. G., ... and Ward, M. N.: Poverty traps and climate risk: limitations and opportunities of index-based risk financing. International Research Institute for Climate and Society. IRI Technical Report 07-02, 2007.

Bisetegne, D., Ogallo, L., andIninda, J.: Rainfall characteristics in Ethiopia, Technical Conference on Meteorological Research in Eastern and Southern Africa, Nairobi, Kenya, 1986.

Block, P., and Rajagopalan, B.: Interannual variability and ensemble forecast of Upper Blue Nile Basin Kiremt season precipitation, Journal of Hydrometeorology, 8(3), 327-343, 2007.

Bonnafous, L., U. Lall, and J. Siegel. An index for drought induced financial risk in the mining industry, Water Resour. Res., 53, 1509–1524, 2017.

Caviedes, C. N.: Emergency and institutional crisis in Peru during El Niño 1982–1983, Disasters, 9(1), 70-74, 1985.

Cid-Serrano, L., Ramírez, S. M., Alfaro, E. J., and Enfield, D. B.: Analysis of the Latin American west coast rainfall predictability using an ENSO index, Atmósfera, 28(3), 191-203, 2015.

Chaffaut, I., Coudrain Ribstein, A., Michelot, J. L., and Pouyaud, B.: Prècipitations d'altitude du Nord-Chili, origine des sources de vapeur et donnèes isotopiques, Bulletin de l'Institut français d'études andines, 27(3), 367-384, 1998.

Chinchay Alza, L.R.: Plan de Gestión de los Recursos Hídricos de la Cuenca Caplina-Locumba, Autoridad Nacional de Agua – ANA, Gobierno del Perú, Lima, Peru, 2015.

Chiock Chang, F. Data made available from OEEE (Office of Economic and Statistical Studies). Annual crop data 1950-2014. MINAGRI Peru, 2016.

Choudhury, A., Jones, J., Okine, A., and Choudhury, R. L.: Drought Triggered Index Insurance Using Cluster Analysis of Rainfall Affected by Climate Change. Journal of Insurance Issues. Vol. 39, No. 2, 169-186, 2016.

Deser, C., and Blackmon, M. L.: On the relationship between tropical and North Pacific sea surface temperature variations, Journal of Climate, 8(6), 1677-1680, 1995.

Dick, W., and Stoppa, A.: Weather Index-based Insurance in Agricultural Development, a Technical Guide. World Food Programme and International Fund for Agricultural Development, 2011.

Efron, B., and Tibshirani, R. An Introduction to the Bootstrap. Chapman & Hall/CRC, 1993.

Efron, B. "Second thoughts on the bootstrap." Statistical Science 18, no. 2: 135-140, 2003.

Eklundh, L., and Pilesjö, P.: Regionalization and spatial estimation of Ethiopian mean annual rainfall, International Journal of Climatology, 10(5), 473-494, 1995.

Enfield, D. B.: Relationships of inter-American rainfall to tropical Atlantic and Pacific SST variability, Geophysical Research Letters, 23(23), 3305-3308, 1996.

Espinoza Villar, J. C., Ronchail, J., Guyot, J. L., Cochonneau, G., Naziano, F., Lavado, W., ... and Vauchel, P.: Spatio-temporal rainfall variability in the Amazon basin countries (Brazil, Peru, Bolivia, Colombia, and Ecuador), International Journal of Climatology, 29(11), 1574-1594, 2009.

Fernandes, K., Baethgen, W., Bernardes, S., DeFries, R., DeWitt, D. G., Goddard, L., ... and Uriarte, M.: North Tropical Atlantic influence on western Amazon fire season variability, Geophysical Research Letters, 38(12), 2011.

Fortaleza, J.: “Boletin de Informacion Estadistica Agraria.” Oficina de Minagri, Puno. 2012.

Fuenzalida, H., and Rutllant, J.: Origen del vapor de agua que precipita sobre el Altiplano de Chile, In Proc II Congreso InterAmericano de Meteorologia, Buenos Aires, Argentina, 1987.

Galarza, F.: “Choices under Risk in Rural Peru.” Staff Paper Series No. 542, University of Wisconsin – Madison, 2009.

Garreaud, R.: Multiscale analysis of the summertime precipitation over the central Andes, Monthly Weather Review, 127(5), 901-921, 1999

Garreaud, R., and Aceituno, P.: Interannual rainfall variability over the South American Altiplano, Journal of Climate, 14(12), 2779-2789, 2001.

Garreaud, R., Vuille, M., and Clement, A. C.: The climate of the Altiplano: observed current conditions and mechanisms of past changes, Palaeogeography, palaeoclimatology, palaeoecology, 194(1), 5-22, 2003.

Glicerio, L. “El cultivo del ulluco en la sierra central del Perú.” Centro Internacional de la Papa – CIP. 2010

Hansen, J. W., Baethgen, W., Osgood, D., Ceccato, P., and Ngugi, R. K.: Innovations in climate risk management: protecting and building rural livelihoods in a variable and changing climate. Journal of Semi-Arid Tropical Agricultural Research, 4(1), 1-38, 2007.

Hellmuth M.E., Osgood D.E., Hess U., Moorhead A. and Bhojwani H. (eds). Index insurance and climate risk: Prospects for development and disaster management. Climate and Society No. 2. International Research Institute for Climate and Society (IRI), Columbia University, New York, USA, 2009.

Helsel, D.R. and Hirsh, R. M.: Statistical Methods in Water Resources: Techniques of Water Resources Investigations, Book 4, Chapter A3, U.S. Geological Survey, 2002.

Higa Eda, L.E. and Chen, W.: Integrated Water Resources Management in Peru, Procedia Environmental Sciences, 2(2010), 340-348, 2010.

Kalnay, E., Kanamitsu, M., Kistler, R., Collins, W., Deaven, D., Gandin, L., ... and Zhu, Y.: The NCEP/NCAR 40-year reanalysis project, Bulletin of the American Meteorological Society, 77(3), 437-471, 1996.

Kayano, M. T., and Andreoli, R. V.: Relations of South American summer rainfall interannual variations with the Pacific Decadal Oscillation, International Journal of Climatology, 27(4), 531-540, 2007.

Khalil, A., Kwon, H., Lall, U., Miranda, J., and Skees, J.: “El Niño-Southern Oscillation – based index insurance for floods: Statistical risk analyses and application to Peru.” Water Resources Research, Vol. 43. 2007.

Kuroiwa, J.M.: Water Resources in Peru: A Strategic View, National Hydraulics Laboratory, National University of Engineering, Lima, Peru, 2007.

Lagos, P., Silva, Y., Nickl, E., and Mosquera, K.: El Niño? Related precipitation variability in Perú. Advances in Geosciences, European Geosciences Union, 14, pp.231-237, 2008.

Lavado-Casimiro, W. S., Felipe, O., Silvestre, E., and Bourrel, L.: ENSO impact on hydrology in Peru, Advances in Geosciences, 33, 33-39, 2013.

Lavado-Casimiro, W. S., Ronchail, J., Labat, D., Espinoza, J. C., and Guyot, J. L.: Basin-scale analysis of rainfall and runoff in Peru (1969–2004): Pacific, Titicaca and Amazonas drainages, Hydrological Sciences Journal, 57(4), 625-642, 2012.

Lenters, J. D., and Cook, K. H.: On the origin of the Bolivian high and related circulation features of the South American climate, Journal of the Atmospheric Sciences, 54(5), 656-678, 1997.

Lenters, J. D., and Cook, K. H.: Summertime precipitation variability over South America: Role of the large-scale circulation, Monthly Weather Review, 127(3), 409-431, 1999.

Ley Nº 28939; Ley que aprueba crédito suplementario y transferencia de partidas en el presupuesto del sector público para el año fiscal 2006, dispone la creación de fondos y dicta otras medidas. El gobierno central del Perú, 2006.

Luo, H., Skees, J., and Marchant, M.: "Weather Information and the Potential for Intertemporal Adverse Selection in Crop Insurance." Review of Agricultural Economics 16, no. 3, 441-51, 1994.

Lynch, B. D.: Vulnerabilities, competition, and rights in a context of climate change toward equitable water governance in Peru's Rio Santa Valley, Global Environmental Change, 22(2), 364-373, 2012.

Mahul, O. and Stutley, C.: "Government Support to Agricultural Insurance: Challenges and Options for Developing Countries; Challenges and Options for Developing Countries." The World Bank Group, Washington, D.C., 2009.

Mallants, D., and Feyen, J.: Defining Homogenous Precipitation Regions by Means of Principal Component Analysis, Journal of Applied Meteorology, 29, 892-901, 1990.

Mandal, A., and Nandi, A.: Hydrological Modeling to Estimate Runoff and Infiltration in Southeastern Appalachian Debris Flow Complex., 3rd North American Symposium on Landslides, Roanoke, Virginia, USA, 2017.

Mantua, N. J., and Hare, S. R.: The Pacific decadal oscillation, Journal of Oceanography, 58(1), 35-44, 2002.

Mantua, N.J., Hare, S.R., Zhang, Y., Wallace, J.M., and Francis, R.C.: A Pacific interdecadal climate oscillation with impacts on salmon production, Bulletin of the American Meteorological Society, 78, 1069-1079, 1997.

Maraun, D.: Bias Correction, Quantile Mapping, and Downscaling: Revisiting the Inflation Issue, J. Climate, 26, 2137–2143, 2013.

Marengo, J. A.: Interannual variability of surface climate in the Amazon basin, International Journal of Climatology, 12(8), 853-863, 1992.

Marengo, J. A., Nobre, C. A., Tomasella, J., Oyama, M. D., Sampaio de Oliveira, G., De Oliveira, R., ... and Brown, I. F.: The drought of Amazonia in 2005, Journal of Climate, 21(3), 495-516, 2008.

Miranda, M. J., and Farrin, K.: Index insurance for developing countries. Applied Economic Perspectives and Policy, 34(3), 391-427, 2012.

Morlet, J., Arens, G., Fourgeau, E., and Giard, D.: Wave propagation and sampling theory – Part I: Complex signal and scattering in multilayered media, Geophysics, 47(2), 203-221, 1982.

Mortensen, E., Wu, S., Notaro, M., Vavrus, S., Montgomery, R., De Piérola, J., Sánchez, C., and Block, P.: "Regression-based season-ahead drought prediction for southern Peru conditioned on large-scale climate variables." Manuscript conditionally accepted. Hydrol. Earth Syst. Sci. Discuss., 10.5194, 2017.

Ogallo, L.: Regional classification of East African rainfall stations into homogeneous groups using the method of principal component analysis, as in Ikeda, S. et a1. (eds), Statistical Climatology. Developments in Atmospheric Sciences, 13. 225-266, Elsevier, Amsterdam, 1980.

Peña Henderson, J.P.: "Seguro Agrario Catastrófico para cultivos de básicos, frutales, hortalizas y forrajes." SBS Nº RG041581-228. La Positiva Seguros. 2016.

Peterson, C.: "Climate-Smart Agriculture in Peru." CSA Country Profiles for Latin America Series, 2nd ed. Washington, D.C. 2015.

Rao, V. B., Cavalcanti, I. F., and Hada, K.: Annual variation of rainfall over Brazil and water vapor characteristics over South America, Journal of Geophysical Research: Atmospheres, 101(D21), 26539-26551, 1996.

Rayner N. A., Parker, D. E., Horton, E. B., Folland, C.K., Alexander, L.V., Rowell, D.P, Kent, E.C., and Kaplan, A.: Global analyses of sea surface temperature, sea ice, and night marine air temperature since the late nineteenth century, Journal of Geophysical Research, 108(D14), 4407, 2003.

Robertson, A., Kirshner, S., Smyth, P., Charles, S., and Bates, B.: Subseasonal-to-inderdecadal variability of the Australian monsoon over North Queensland, Quarterly Journal of the Royal Meteorological Society, 132, 519-542, 2006.

Robertson, A., Moron, V., and Swarinoto, Y.: Seasonal predictability of daily rainfall statistics over Indramayu district, Indonesia, International Journal of Climatology, 29, 1449-1462, 2008.

Robles, M.: "Catastrophic Crop Insurance – Peru." International Food Policy Research Institute. 2015.

Rojas-Suarez, Liliana, Currency Substitution and Inflation in Peru (May 1992). IMF Working Paper, Vol., pp. 1-46, 1992.

Rutllant, J., and Ulriksen, P.: Boundary-layer dynamics of the extremely arid northern part of Chile, Boundary-Layer Meteorology, 17(1), 41-55, 1979.

Sadoff, C., and Muller, M.: Water management, water security and climate change adaptation: early impacts and essential responses, Stockholm: Global Water Partnership, 2009.

Silva Dias, P. L., Schubert, W. H., and DeMaria, M.: Large-scale response of the tropical atmosphere to transient convection, Journal of the Atmospheric Sciences, 40(11), 2689-2707, 1983.

Skees, J. and Collier, B. New approaches for index insurance. New approaches for index insurance. International Food Policy Research Institute (IFPRI), 2020 vision briefs, 2010.

Skees, J., Hartell, J., and Murphy, A.: "Using Index-Based Risk Transfer Products to Facilitate Micro Lending in Peru and Vietnam." Amer. J. Agr. Econ. 89. 2007

Stone, M.: Cross-validation: a review, Statistics: A Journal of Theoretical and Applied Statistics 9.1, 127-139, 1978.

Svensson, C.: Seasonal river flow forecasts for the United Kingdom using persistence and historical analogues, Hydrol. Sci. J., 61(1), 19–35, 2016.

Takahashi, K., Montecinos, A., Goubanova, K., and Dewitte, B.: ENSO regimes: Reinterpreting the canonical and Modoki El Niño, Geophysical Research Letters, 38(10), 2011.

Tapley Jr, T. D., and Waylen, P. R.: Spatial variability of annual precipitation and ENSO events in western Peru, Hydrological Sciences Journal, 35(4), 429-446, 1990.

Torrence, C., and Compo, G. P.: A practical guide to wavelet analysis, Bulletin of the American Meteorological Society, 79(1), 61-78, 1998.

Trenberth, K. E.: The definition of El Niño, Bulletin of the American Meteorological Society, 78(12), 2771-2777, 1997.

Trenberth, K. E., and Hurrell, J. W.: Decadal atmosphere-ocean variations in the Pacific, Climate Dynamics, 9(6), 303-319, 1994.

Trenberth, K.E. and National Center for Atmospheric Research Staff (Eds). Last modified 02 Feb 2016. "The Climate Data Guide: Nino SST Indices (Nino 1+2, 3, 3.4, 4; ONI and TNI).", 2016.

Ugarte, A.: Síntesis del Plan de Gestión de los Recursos Hídricos – Cuencas: Caplina, Sama, y Locumba, Consejo de Recursos Hidricos de Cuenca Caplina-Locumba, Tacna, Peru, 2012.

Urby, H., McEntire, D, and Peters, E. Peru: An Andean Country with Significant Disaster and Emergency Management Challenges. Us. Department of Homeland Security, FEMA, 2010.

Valdivieso, M.,: “Producción Orgánica de Cultivos Andinos; Manual Técnico.” Food and Agriculture Organization of the United Nations. 2010.

Van Loon, A. F.: Hydrological drought explained, Wiley Interdiscip. Rev. Water, 2(4), 359–392, 2015.

Velazco, J. Agricultural Production in Peru (1950-1995): Sources of Growth. Chapter 6, Agricultural Investment and Productivity in Developing Countries. FAO ECONOMIC AND SOCIAL DEVELOPMENT PAPER 148, 2001.

Vera, R.: “Country Pasture/Forage Resource Profiles: Peru.” Food and Agriculture Organization of the United Nations. 2006.

Vizy, E. K., and Cook, K. H.: Relationship between Amazon and high Andes rainfall, Journal of Geophysical Research: Atmospheres, 112(D7), 2007.

von Storch, H., and Zwiers, F. W.: Statistical analysis in climate research, Cambridge University Press, 2001.

Vuille, M.: Atmospheric circulation over the Bolivian Altiplano during dry and wet periods and extreme phases of the Southern Oscillation, International Journal of Climatology, 19, 1579-1600, 1999.

Vuille, M., Bradley, R. S., and Keimig, F.: Interannual climate variability in the Central Andes and its relation to tropical Pacific and Atlantic forcing, Journal of Geophysical Research: Atmospheres, 105(D10), 12447-12460, 2000.

Walpole, R. E., Myers, R. H., Myers, S. L., and Ye, K.: Probability and statistics for engineers and scientists (Vol. 9), New York: Macmillan, 2012.

Wang, C., and Enfield, D.B.: The tropical Western Hemisphere warm pool, Geophysical Research Letters, 28, 1635-1638, 2001.

Wang, C., and Enfield, D. B.: A further study of the tropical Western Hemisphere warm pool, Journal of Climate, 16(10), 1476-1493, 2003.

Wang, C., and Fiedler, P. C.: ENSO variability and the eastern tropical Pacific: a review, Progress in Oceanography, 69(2), 239-266, 2006.

Wang, L., Chen, W., and Huang, R.: Interdecadal modulation of PDO on the impact of ENSO on the East Asian winter monsoon, Geophysical Research Letters, 35(20), 2008.

Wilks, D. S.: Statistical methods in the atmospheric sciences (Vol. 100), Academic Press, 2011.

World Bank Group: "Agricultural Insurance in Latin America; Developing the Market." International Bank for Reconstruction and Development. 2015.

World Bank Group: Managing agricultural production risk: Innovations in developing countries. Washington, DC: Agriculture and Rural Development Department (ARD), World Bank, 2005.

World Bank Group: "Peru: A Comprehensive Strategy for Financial Protection against Natural Disasters." International Bank for Reconstruction and Development. 2016.

Wu, S., and Liu, Q.: Some problems on the global wavelet spectrum, Journal of Ocean University of China, 4(4), 398-402, 2005.

Wu, S., Notaro, M., Vavrus, S., Mortensen, E., Montgomery, R., De Piérola, J., Sánchez, C., and Block, P. The Efficacy of Tendency and Linear Inverse Models to Predict southern Peru Summertime Precipitation. Manuscript conditionally accepted. Intl. JOC, Vol., 2017.

Xu, C.: Climate Change and Hydrologic Models: A Review of Existing Gaps and Recent Research Developments. Water Res. M., 13, 369-382. 1999.

Yoon, J. H., and Zeng, N.: An Atlantic influence on Amazon rainfall, Climate Dynamics, 34(2-3), 249-264, 2010.

Zeng, N., Yoon, J. H., Marengo, J. A., Subramaniam, A., Nobre, C. A., Mariotti, A., and Neelin, J. D.: Causes and impacts of the 2005 Amazon drought, Environmental Research Letters, 3(1), 014002, 2008.